3-10-2015

Synthesis, Characterization, and Electrochemical Properties of Polyaniline Thin Films

Soukaina Rami
University of South Florida, soukaina@mail.usf.edu

Synthesis, Characterization, and Electrochemical Properties of Polyaniline Thin Films

by

Soukaina Rami

A thesis submitted in partial fulfillment
of the requirements for the degree of
Master of Science in Mechanical Engineering
Department of Mechanical Engineering
College of Engineering
University of South Florida

Co-Major Professor: Manoj Ram, Ph.D.
Co-Major Professor: Ashok Kumar, Ph.D.
Arash Takshi, Ph.D.

Date of Approval:
March 10, 2015

Keywords: conjugated, polymers, electrochemistry, self-assembly, deposition

ACKNOWLEDGMENTS

I would like to thank my supervisors, Dr. Manoj K. Ram and Dr. Ashok Kumar for not only their guidance and wisdom, but also for their patience throughout my schooling at USF. I also find great pleasure to acknowledge Dr. Arash Takshi for his continued support in preparation of this manuscript. I would like to acknowledge my supporting labmates, especially Saumya Sharma for helping me with the SEM imaging and Mike Mccroy for the XRD measurements. Last but not least, I would to thank my family for always supporting me and believing me, and my dear friends for always being there for me.

TABLE OF CONTENTS

LIST OF TABLES

LIST OF FIGURES

ABSTRACT

Conjugated polymers have been used in various applications (battery, supercapacitor, electromagnetic shielding, chemical sensor, biosensor, nanocomposite, light-emitting-diode, electrochromic display etc.) due to their excellent conductivity, electrochemical and optical properties, and low cost. Polyaniline has attracted the researchers from all disciplines of science, engineering, and industry due to its redox properties, environmental stability, conductivity, and optical properties. Moreover, it is a polymer with fast electroactive switching and reversible properties displayed at low potential, which is an important feature in many applications. The thin oriented polyaniline films have been fabricated using self-assembly, Langmuir-Blodgett, in-situ self-assembly, layer-by-layer, and electrochemical technique. The focus of this thesis is to synthesize and characterize polyaniline thin films with and without dyes. Also, the purpose of this thesis is to find the fastest electroactive switching PANI electrode in different electrolytic medium by studying their electrochemical properties. These films were fabricated using two deposition techniques: in-situ self-assembly and electrochemical deposition. The characterization of these films was done using techniques such as Fourier Transform Infrared Spectroscopy (FTIR), UV-spectroscopy, Scanning Electron Microscope (SEM), and X-Ray Diffraction (XRD). FTIR and UV-spectroscopy showed similar results in the structure of the polyaniline films. However, for the dye incorporated films, since there was an addition in the synthesis of the material, peak locations shifted, and new peaks corresponding to these materials appeared. The 1 layer PANI showed compact film morphology, comparing to other PANI films, which displayed a fiber-like structure. Finally, the electrochemical properties of these thin films were studied

using cyclic voltammetry (CV), chronoamperometry (CA), and electrochemical impedance spectroscopy (EIS) in different scenarios. These scenarios included the study in different acid based electrolytes and different gel based electrolytes. The ultra-thin self-assembled PANI films were shown to have a faster switching time, especially for the 1 layer PANI, whereas the color contrast could be observed for the film containing the dye molecule. Also, HCl based electrolyte gave the best electrochemical reversibility compared to other acids used. For the gelatin and PVA based electrolytes, having the same concentration, the results were similar. Hence, the change in the electrolyte consistencies, from liquid to semi-solid, did not change the electrochemical properties of the films. Finally, in the EIS, it was shown that these PANI thin films exhibit a pseudo-capacitance behavior, and as the film thickness grew, the capacitance increased.

CHAPTER 1. INTRODUCTION

1.1 Conjugated Electrochromic Materials

Polymeric materials have been considered as insulators for decades; however, it has been found that these polymers could exhibit conductive properties by undergoing a redox reaction called doping. By doping, the conductivity of the semiconductor can increase by several orders in magnitude. These polymers are, hence, called conjugated, because of the delocalization of the π-electron along their backbone [1]. The electrical properties of conjugated polymers are dependent on the redox state, which alternates the polymers' electronic structure. As such, the polymer gains the property of changing from insulating to a conductive material, which is known as the doping process [2]. There are two types of doping: P-type doping and N-type doping. N-type doping tends to lose an electron, which increases the conductivity of the material and is referred as the reduction of the polymer. On the other hand, P-type doping is referred as the oxidation of the polymer and is the most used type of doping in the semiconducting industry. To achieve this change in the material's property, a chemical process can be induced by adding an oxidizer or reducer, or by using an electrochemical synthesis [3]. π-conjugated polymers have attracted attention for many applications in EMI shielding [4], battery [5], supercapacitor [6], chemical sensor [7], biosensor [8], nanocomposite [9], light-emitting-diode [10], electrochromic display [11], because of their high electrical conductivity when doped, thermal stability, oxidation resistivity, high volume, and low cost. The common conjugated polymers are polypyrrole (PPy), polythiophene (PT), and polyaniline (PANI) [12]. Some of these polymers are shown in figure 1.

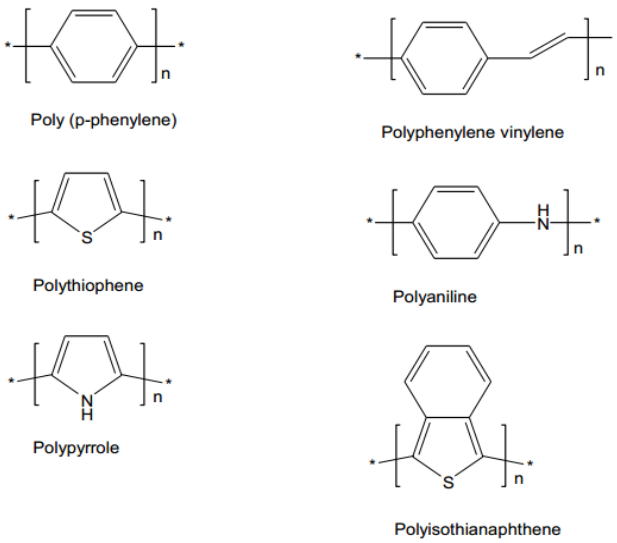

Figure 1 Chemical structure of conjugated polymers. Reproduced with permission [12]

Figure 2 shows the conductivity scale of different conjugated polymers and metals. Polyaniline (in its emeraldine form) is shown as the least conductive material in the scale, comparing to other polymers such as polypyrrole and polyacetylene.

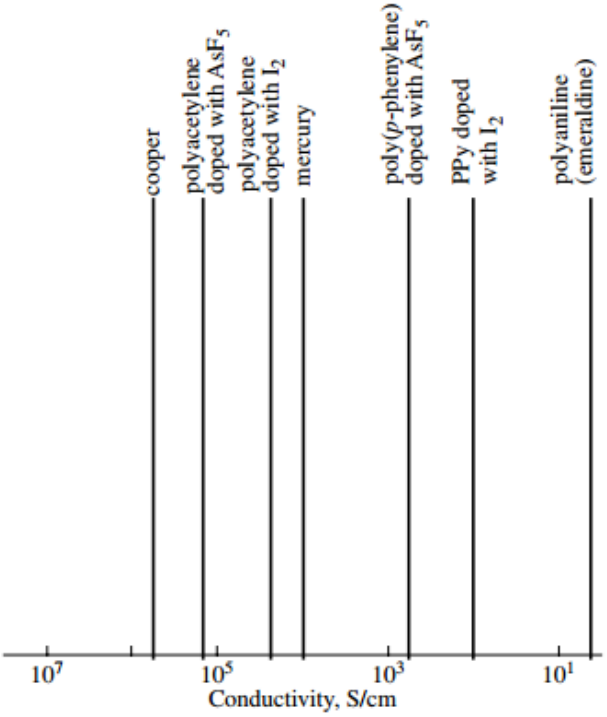

Figure 2 Conductivity ladder of different materials. Reproduced with permission [13]

As mentioned previously, conjugated polymers have doped and dedoped forms. The dedoped form constitutes of a π-bonding orbital (valence band(VB)-highest occupied energy level), and a π^*-antibonding orbital (conduction band(CB)-lowest occupied energy level) [14]. The distance between these two orbitals is known as the energy band gap E_g. No electron exists in this region, and thus allows many intrinsic properties of conducting polymers to be exacted. For metals, there is no band gap, and for the semiconductors, the distance between the two orbitals is narrow. For the case of insulators, there is a wide band gap as shown in figure 3.

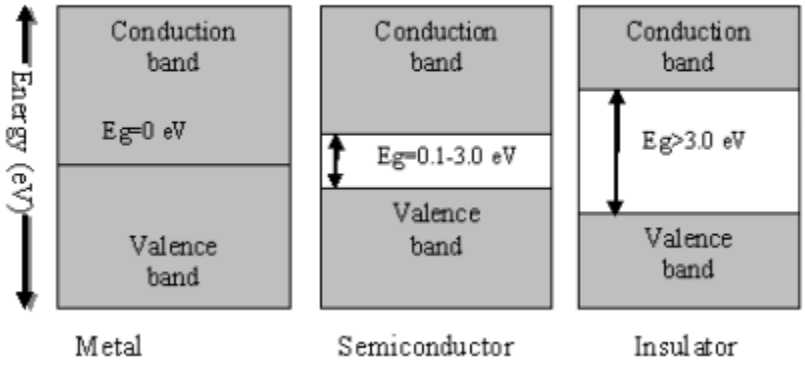

Figure 3 Electronic band structures for different solid states. Reproduced with permission [12]

Table 1 summarizes the bandgap for different types of inorganic and organic semiconductors [2].

Table 1 Bandgap for different semiconductors.

Name	Bandgap(eV)	Name	Bandgap
Silicon	1.1	Polyacetylene	1.7
Germanium	0.7	Polypyrrole	3.2
Cadium Sulfide	2.5	Polythiophene	2.0
Zinc Oxide	3.3	Polyparaphenylene	3.5

Note the conductivity of these semiconductors is dependent on the formation of the mobile charge carriers, which is how the orbitals are filled. When the orbitals are filled, there is no

movement, and hence it is in an insulating form. On the other hand, when there is a movement of electrons from the VB to the CB for conjugated polymers, electron holes are created. They do not delocalize the polymer, but there is a distortion happening in the lattice, which is best known as a polaron (radical cation). This energy created lies between the CB and VB, and this radical cation carries a ½ spin and a negative charge.

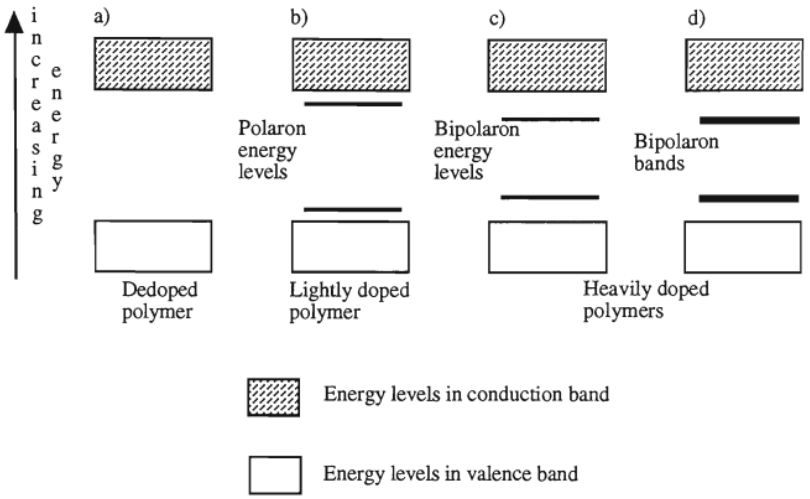

Figure 4 Polaron/bipolaron formation in conducting polymers. Reproduced with Permission [2]

When a second electron (e^-) is removed or added to the chain of a pre-existing polaron, a bipolaron is created due to the reduction in dimerization parameter. This dimerization can tend to reduce the total energy. The presences of these polarons/bipolarons are dependent with the doping level in conjugated polymer. When a high dopant is used, the polarons/bipolarons overlap with the dopant ion, which causes the overlapping of VB and CB. Figure 4 shows the formation of the polaron/bipolaron band before and after doping the polymers [2].

Figure 5 shows the properties and applications of polymers in different states from insulator-semiconductor-conductor states. There is a relationship between the properties of the polymers

and the application in which it has been used. For instance, semiconductor polymers can be used as Schottky rectifier, field-effect resistors, or light-emmiting diode solar cells. On the other hand, conductor polymers can be used as an electromagnetic interference shielding or a microwave absorbing material. Then the doping/de-doping process, which goes from insulating to conducting, can create a color change, which can be used for the application of electrochromic devices.

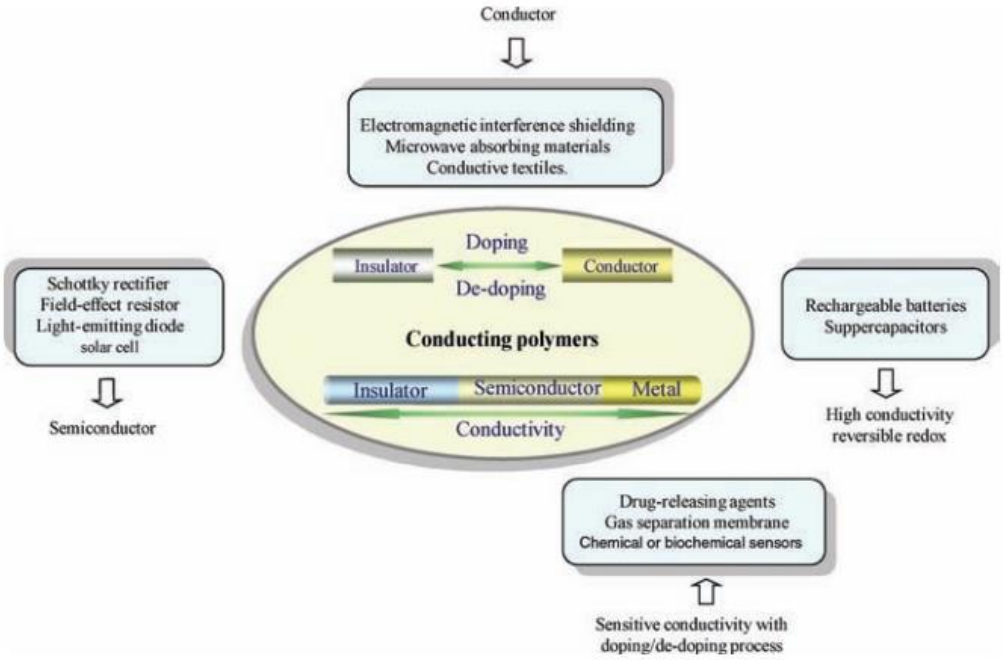

Figure 5 Properties and application of conductive polymers. Reproduced with permission [3]

1.2 Polyacetylene

Polyacetylene (PA) were first synthesized by Natta et al in 1958 and resulted in a black powder [15]. In 1974, it was further studied and proven PA had a strong mechanical property [16]. In 1977, Chiang and al further researched the synthesized polymer by Hirakata et al. and increased its magnitude by an order of 13 by doping it [17]. Different dopants can be used to synthesize PA, such as p-type dopants, which increase the conductivity by high order of magnitude similar

to the one exhibited by metals such as copper [18]. Some of these dopants are bromine, iodine, and arsenic pent fluoride. However, n-type dopants (e.g. lithium and potassium) can also be used, but the conductivity of the polymer doesn't increase significantly [19]. PA advantages are its simple molecular structure, abundant materials necessary for its synthesis, and its high conductivity using different dopants. However, PA exhibits defects with its π bonds, which makes it very hard to control its synthesis. Moreover, PA does not display reversible transformations like other conjugated polymer (PT, PPy, and PANI), because it is sensitive to H_2O and O_2. Also, some drawbacks of PA are its insolubility [20]. Due to these many drawbacks, PA has no commercial use, and scientists have given more importance towards efficient polymers.

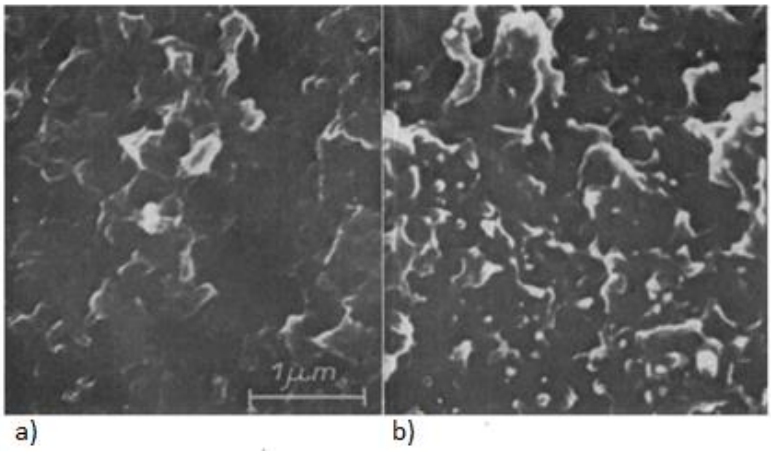

Figure 6 SEM images of doped PA films. a)H_2SO_4 b)$BiCl_2$. Reproduced with permission [21]

Figure 6 shows the morphology of PA films doped with H_2SO_4 and $BiCl_2$. The film was prepared by using the method done by Ito et al. [16]. The film, for both dopants, shows similar morphology, which corresponds to a fibrillary shape [21].

Figure 7 shows the cyclic voltammetry of polyacetylene in 1M $LiClO_4$ at a scan rate of 50 mV/s. The PA film exhibits one anodic and one cathodic peak. The peaks are symmetrical; however, the cathodic peak of PA is much smaller and broader than the one displayed by the anodic peak.

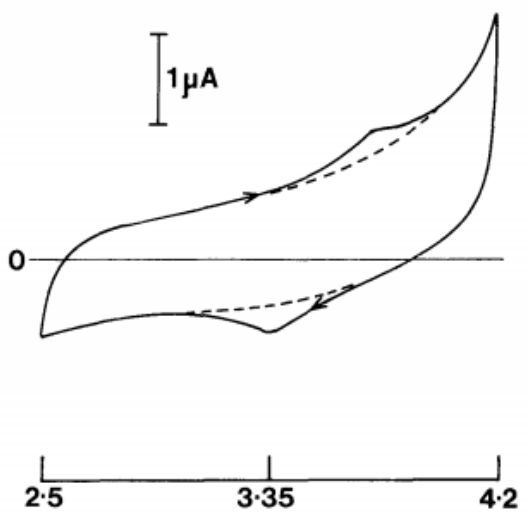

Figure 7 CV of 1.1 ng of $(CH)_x$ in 1M $LiClO_4$ at 50 mV/s (dashed line) background scan. Reproduced with permission [21]

1.3 Polypyrrole

Polypyrrole (PPy) was discovered in 1963 by Bolto et al. as a conducting polymer with great electrical properties [22]. It was in 1983 that Diaz and Hall have synthesized PPy, making its conductivity in the semiconductor range [23]. By oxidizing the monomer pyrrole, one can obtain a black powder. Doped PPy films can display a dark blue or black color depending on many factors, such as the degree of polymerization and the thickness of the film obtained. The lightly doped polypyrrole has a lime green/turquoise color, and the undoped polypyrrole has a light yellow color. The bandgap E_g of PPy is around 3.2 eV. If the bandgap has a value larger than 3 eV, the polymer will display a transparent color [24]. PPy is one of the most electrochemically synthesized polymer, especially amongst heterocyclic conjugated polymers [25]. It has the unique property of being synthesized using an aqueous solution. Polythiophene and polyaniline

do not share the same property. Thiophene is synthesized from an organic solvent, and aniline requires an acidic medium [13]. However, the polymerization of PPy has nucleophile sensitivity in the surface of the electrode. Some of the poor nucleophilic solvent that can be used are acetonitrile, propylene carbonate, methylene chloride, and tetrahydrofuran [26]. PPy can also be synthesized in nucleophilic solvents, but a pyrotic acid has to be added in the electrolyte to decrease the solvent's neucleophilicity. Some of these solvents are dimethyl sulfoxide and dimethyl formamide. PPy conductivity can range from 10^2-10^3 S/cm [27].

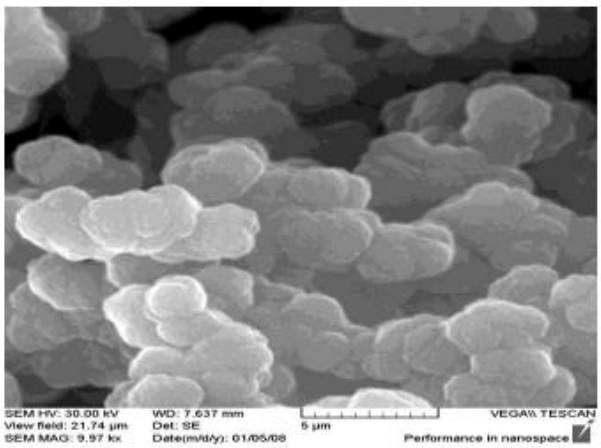

Figure 8 SEM images of polypyrrole thin film. Reproduced with permission [28]

The morphological structure of a 1 µm PPy thin film consists of 3D structure with negligible crystallinity, and it contains a globular-like shape, as shown in figure 8. The thin film was deposited electrochemically using a three-point electrode on a platinum rotating disk in 0.1M of $LiBF_4$.

It can be used as a biomaterial for the application of biomedical implants. Also, PPy can be used as an antistatic coating for corrosion protection in rechargeable batteries, gas sensors, Schottky diodes, and electrochromic displays [29]. However, disadvantages of PPy are its low mechanical

strength, making it a fragile material, and its limited solubility in most of the organic solvents [30].

The cyclic voltammetry for 1 µm PPy thin film in an electrolyte consisting of 1M lithium perchlorate ($LiClO_4$) is displayed in figure 9 at two different scan rate of 10 mV/sec and 20 mV/sec. PPy undergoes a redox reaction with one anodic and one cathodic peak. The thin film displays an electrochromic behavior from a dark brown to a light yellow. The cyclic voltammetry, however, is not symmetrical, but displays a quasi-reversible behavior.

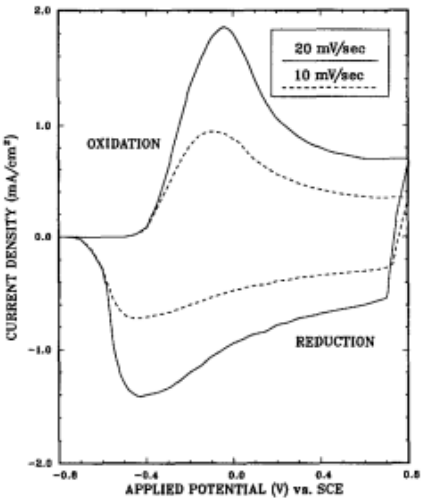

Figure 9 Cyclic voltammetry for 1 µm PPY in 1M $LiClO_4$. Reproduced with permission [31]

1.4 Polythiophene

Polythiophene (PT) was discovered and chemically synthesized in the 1980s by two groups (T.Yamamoto et al. and J.W.P Lin et al.) [32, 33]. PT has excellent electrochromic properties. It displays a dark blue color when heavily undoped, purple when lightly doped, and red when undoped. It has a bandgap of E_g=2.0 eV [24]. Depending on the dopant used, the conductivity of PT can reach up to 1000 S/cm [34]. PT shares the same characteristic as PPy, as it is a

heterocyclic polymer. It contains a heterocyclic four members with sulfur atom [35]. It is insoluble even if a small concentration is used in THF. It has a very limited range of solvent that can be used, such as a mixture of arsenic trifluoride and arsenic pent fluoride [36]. PPy and PT both show porous properties. Iodine doped PT has been found to have the highest conductivity [35]. Moreover, It has been found that PT doped with $FeCl_3$ increases crystallinity [37]

PTs are regarded as the most thermally and environmentally stable conjugated polymer. Their application can go from electrical conductors, LEDs, smart windows, sensors, antistatic coatings, biomaterials, and nanoswitches [38].

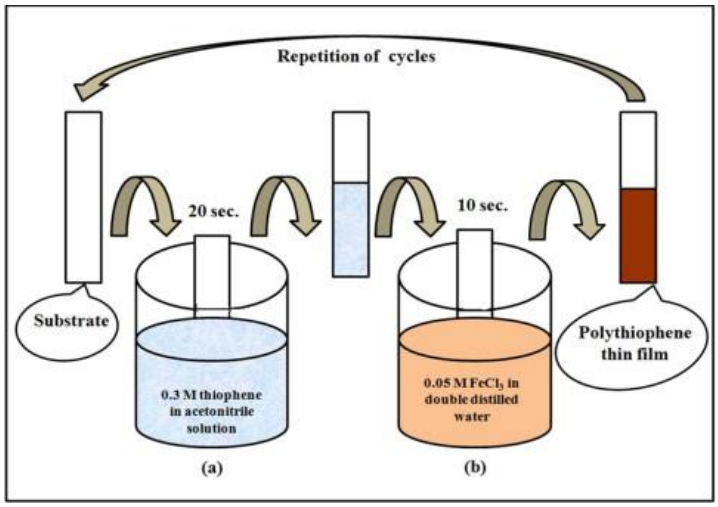

Figure 10 SILAR method for PT film deposition. Reproduced with permission [39]

Patil et al. work has been studied to understand the properties of polythiophene [39]. The thin film was deposited on a glass substrate using the successive ionic layer adsorption and reaction method (SILAR), which is a simple and inexpensive technique for film deposition. Figure 10 shows the schematic of this method for creating a PT film. The substrate was dipped for 20 second in a solution consisting of 0.3 M of thiophene in acetonitrile solution (cation precursor, where the adsorption of thiophene on the glass substrate occurs), and then was dipped for 10 sec

in a solution containing 0.05M of $FeCl_3$ in DI water. The $FeCl_3$ is an oxidant (ionic precursor, and the thin film darkens to a dark red color).

To understand the morphology of the PT films, the SEM images were studied as shown in figure 11, PT films have a uniform surface with some coalesced grains randomly distributed.

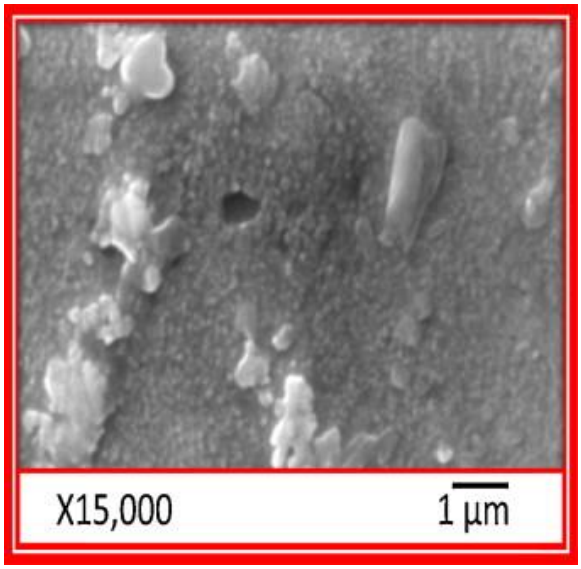

Figure 11 SEM images for polythiophene. Reproduced with permission [39]

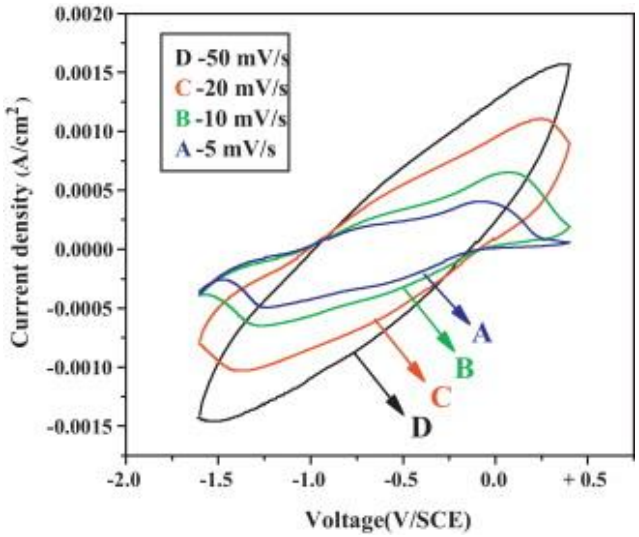

Figure 12 CV of PT thin film in 0.1 M $LiClO_4$. Reproduced with permission [39]

Finally, the cyclic voltammetry from the same paper was studied to understand the electrochemical properties of PT films as shown in figure 12. The electrolyte used was 0.1 $LiClO_4$ in propylene carbonate. The voltage range was from -1.6 to 0.4V/SCE. The peaks are barely noticeable at higher scan rates; however, when the scan rate decreases, a redox peak is noticeable at 20 mV/s and 50 mV/s. Also as the scan rate increases, the potential increases as well.

1.5 Polyaniline

1.5.1 Introduction to Polyaniline

Polyaniline (PANI) is an organic semiconductor discovered in 1834 by Runge and was known as "aniline black". It was further researched by Letheby who discovered the ability of aniline to produce a blue substance [40]. It was until 1912 that Green and Woodhead discovered the different forms of aniline from insulating to conducting [41]. Polyaniline is also known as a synthetic polymer. Figure 13 below is the general formula of polyaniline [12].

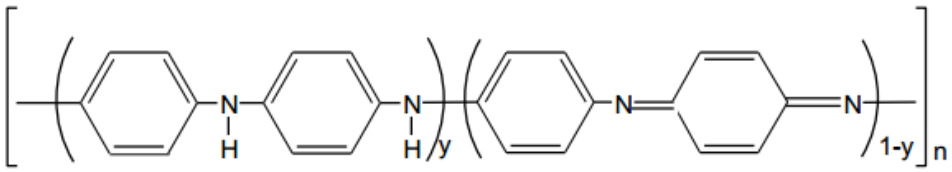

Figure 13 Polyaniline general formula. Reproduced with Permission [12]

The doping of the polymer involves electron and proton transfer. Polyaniline has three different oxidation states [42, 43]. From figure 13:

- y=1 corresponds to leucoemeraldine, which is the fully reduced form of undoped PANI.
- y=0.5 for emeraldine, which is the intermediate oxidation state of PANI.

- y=0 for pernigraniline, which is the fully oxidized form of undoped PANI.

Table 2 below summarizes all the six different forms of PANI from base to salt [44]. These forms change depending on the protonation and the oxidation mechanism of PANI.

Table 2 Different forms of PANI. Reproduced with Permission [44]

Polymer	Oxidation state	Color	Electrical Conductivity
Leucoemeraldine salt	Unoxidized protonated polymer	Transparent yellow	Insulator- 10^{-12} Scm^{-1}
Leucoemeraldine base	Unoxidized deprotonated polymer	Yellow	Insulator-10^{-12} Scm^{-1}
Emeraldine base	Partially oxidized deprotonated polymer	Blue	Insulator-10^{-12} Scm^{-1}
Emeraldine salt	Partially oxidized protonated polymer	Green	Conductor<10^{-4}-10^{2} Scm^{-1}>
Pernigraniline base	Fully oxidized deprotonated polymer	Violet	Insulator 10^{-12} Scm^{-1}
Pernigraniline Salt	Fully oxidized protonated polymer	Violet	Insulator 10^{-12} Scm^{-1}

PANI shows ease in synthesis at low cost, and possesses excellent conductivity, electrochemical and optical properties. Besides, PANI is environmentally stable and thermally stable. PANI is unique for the fact it can change into a non-conducting state of emeraldine and pernigraniline with change in electronic structure by simply treating it with various chemicals. This

transformation can be done by introducing electrons in the PANI structure and reducing the N atom, removing the polaron-stabilizing acid.

Polyaniline can be synthesized using several methods. This thesis concentrates on two different synthesis methods which are electrochemical [2] and chemical polymerization [45]. Both these methods consist of an oxidative polymerization of the monomer (aniline) in an aqueous acid (hydrochloric acid). As a result, an oligomer is formed, which is oxidized again to form a polymer chain.

Electrochemical deposition involves the polymerization of the monomer in an electrolytic medium. A three point electrode is used. The set up consists of a counter electrode (platinum), a reference electrode (Ag/Ag chloride electrode), and a working electrode (ITO or FTO glass slide). The polymerization can be carried out using a potentiostatic, potentiodynamic, or galvanostatic method [46]. The only difference is that the redox driving force in electrochemical doping is provided by an external voltage source; whereas, chemical oxidation utilizes oxidants to precipitate the chemical reaction [38, 47]. For chemical polymerization to occur, an oxidizing agent has to be incorporated within the acidic medium. In this case, an oxidant (ammonium peroxydisulfate-APS) is used in the chemical polymerization; its oxidation potential is E_0=1.94 V. Cation radicals are formed by the oxidation of the monomers produced by APS. These radicals react with other monomers, which results in the creation of oligomers (insoluble polymers). One of the advantages of chemical synthesis is its capability to produce bulk quantities of thin films. On the other hand, the disadvantage is a narrow range of chemical oxidants available for the purpose of chemical polymerization [46].

1.5.2 Polymerization Mechanism

This section is covering a general mechanism of polymerization of PANI. PANI's structure involves irregular nitrogen groups and phenyl rings. This structure creates a zigzag pattern, where a π electron cloud surrounds the pattern. The polymerization process starts by an electron transfer of the aniline nitrogen atom as shown in figure 14. This transfer forms a radical cation in the polyaniline conjugated polymer [48].

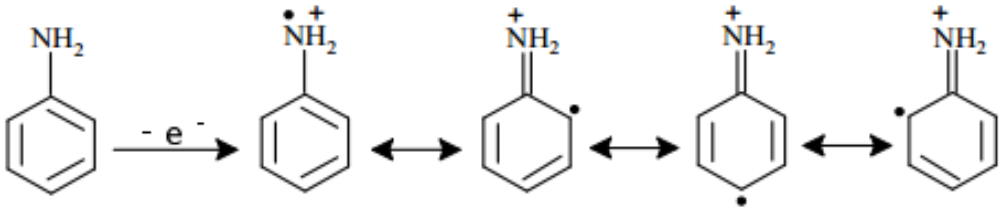

Figure 14 Structure of the electron transfer of the aniline nitrogen atom. Reproduced with permission [48]

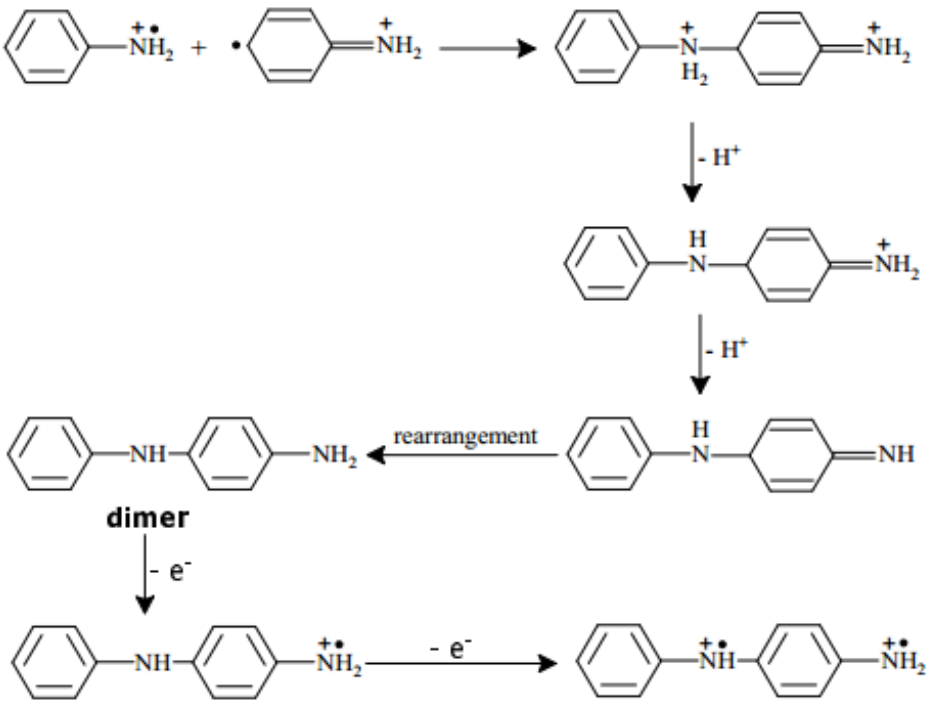

Figure 15 Reaction of the radical cation to form the radical dimer. Reproduced with permission [48]

The formed radical cation reacts with its resonant form in a “head to tail” manner, which forms an oxidized radical cation dimer (figure 15). The polymerization ends by the creation of a trimmer, which is the result of the reaction of the formed radical with the radical monomer or dimer. The above step keeps on following the same pattern until a long chain of PANI is formed as shown in figure 16.

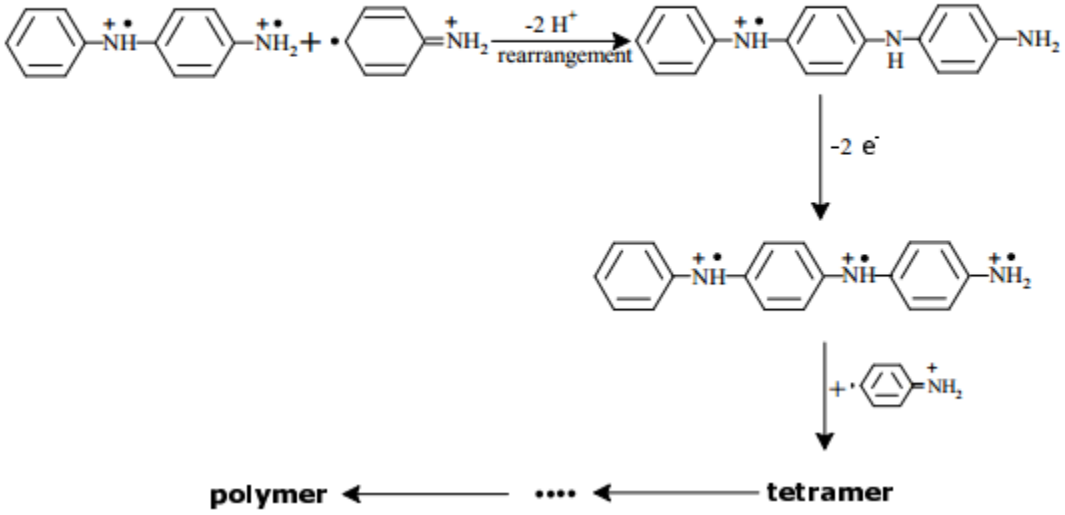

Figure 16 Schematic of the formation of polyaniline. Reproduced with permission [12]

1.5.3 Properties of Polyaniline

1.5.3.1 PANI Switching Properties and Electrochemical Properties

PANI exhibits color switching properties when undergoing a redox reaction. Figure 17 shows these color changes for a PANI thin film. The experiment was done by oxidizing PANI at 1 M HCl. PANI has a pH dependency for each of the oxidation states of PANI. This dependency is a result of the addition of an acid or base when the emeraldine salt is formed.

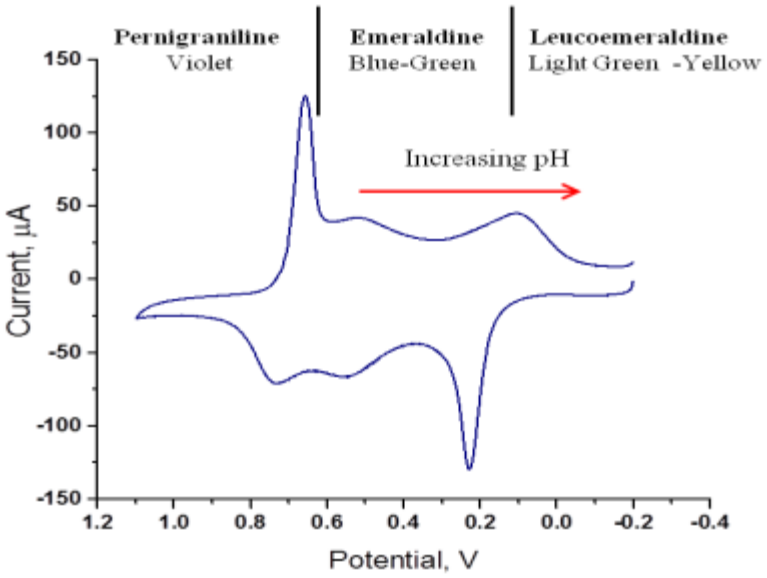

Figure 17 Cyclic voltammetry of PANI thin film on platinum in 1M Hcl at a scan rate of 100mV/s. Reproduced with permission [12]

When in reduction state, PANI thin film exhibits a yellow color to transparent as shown in figure 18a, which corresponds to the state of leucoemeraldine. The green color (emeraldine salt) (figure 18b) is noticed when the film is undergoing oxidation. Polyaniline hydrochloride converts to a non-conducting blue emeraldine base (EB), which is considered the most applicable form of PANI. This form is obtained when treated with ammonium hydroxide. When the temperature reaches its maximum, the emeraldine base converts to a conductive green emeraldine salt (ES). The ES form of PANI has the highest conductivity (similar to a semiconductor) amongst other forms of PANI. Figure 19 shows these same properties for the dye incorporated thin films. Figure 19a and b shows the switching properties for the Rhodamine B/PANI film and PANI/Prussian Blue film consecutively.

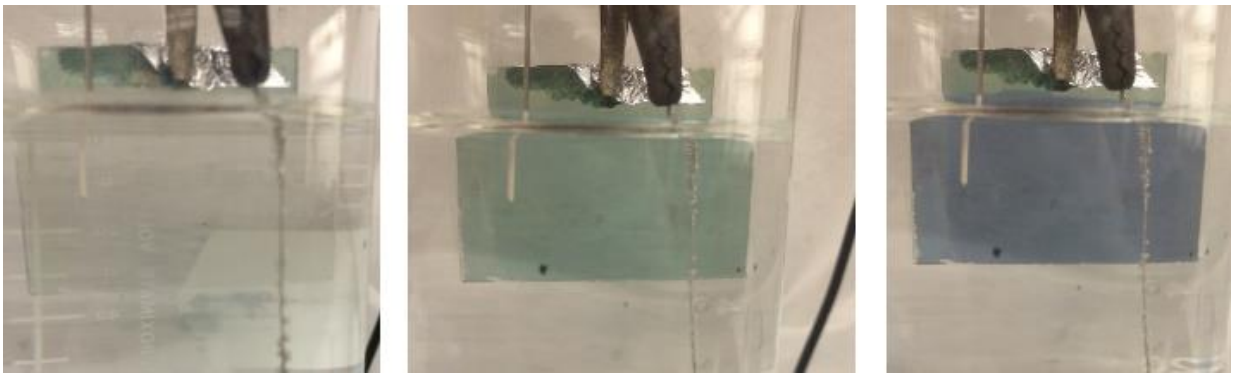

a) b) c)

Figure 18 PANI undergoing cyclic voltammetry. a) PANI in the reduction state b) and c) in the oxidation state

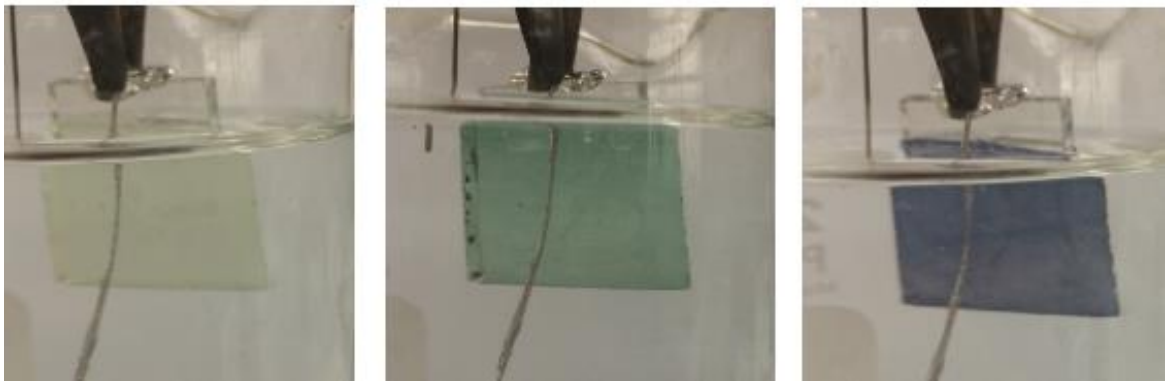

a)

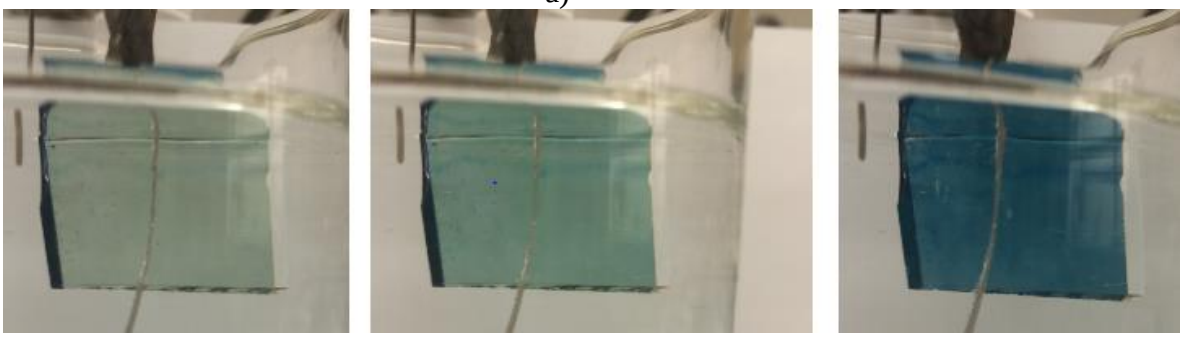

b)

Figure 19 Different states of dye incorporated films. a) redox reaction of rhodamine B/PANI b) redox reactions of prussian blue/PANI

1.5.3.2 Electrical Properties and Optical Properties

PANI has an electrical property that can reversibly be controlled by charge transfer doping. PANI has an electrical conductivity between 10^{-10} and 10^{2} ohm [48]. Figure 20 shows the band

gaps for each redox states of PANI [49]. Emeraldine salt has three characteristic bands at 330 nm, 430 nm, and a broad band at 800 nm. The 330 nm is due to π-π^* transition, 430 nm is due to π-polaron band, and the wide 800 nm is due to the π^*-polaron /bipolaron band. The emeraldine base state of polyaniline exhibits a π-π^* band at 600 nm, which is due to charge transfer that occurs between the adjacent imine-phenyl-amine and the quinoid ring. The maximum absorption is around 2.1 eV; as for pernigraniline base, it is around 2.3 eV with two bands at around 320 nm and 530 nm corresponding to π-π^* band and Peierl band gap consecutively [50].

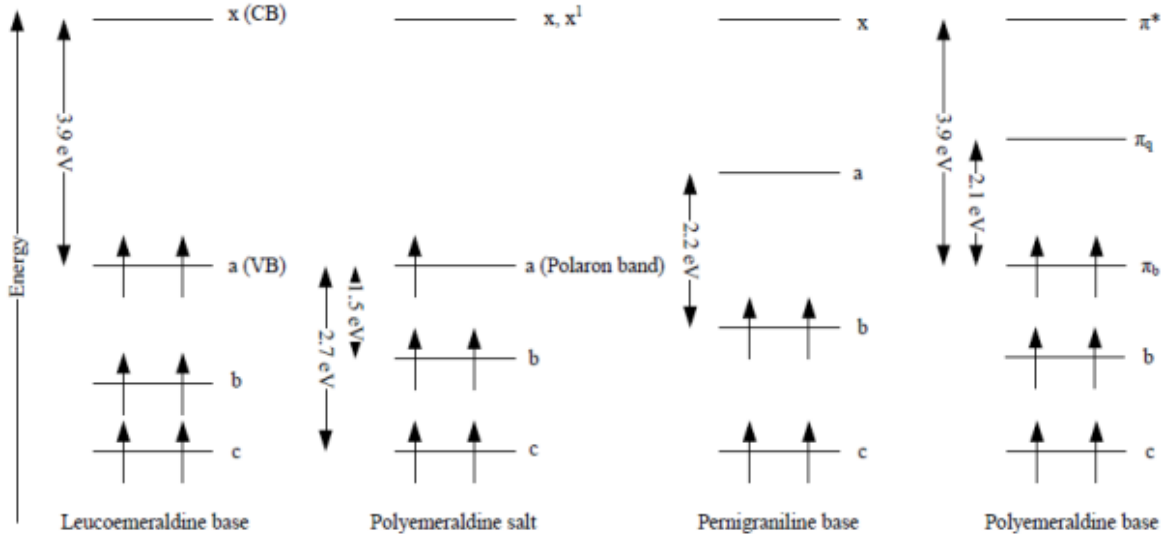

Figure 20 Band gap for different redox state of PANI. Reproduced with permission [49]

1.5.3.3 Morphology of Polyaniline

Polyaniline has a different morphology than the one observed by other polymers. It consists of a rod-like morphology, where the rods diameter is around 500 nm as shown in Figure 21 [28]. The rod-like structure is dependent on the concentration of polyaniline. This similar morphology was not observed when a low concentration of PANI was used.

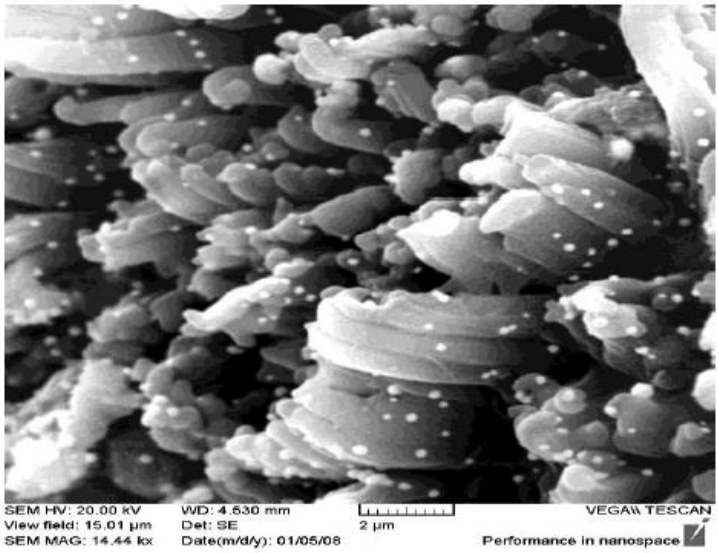

Figure 21 SEM images for polyaniline thin films. Reproduced with permission [28]

1.5.4 Applications of Polyaniline

PANI has been used for antistatic coating [51], electrodes in batteries [52],and electrochromism [53]. These are couple of applications for polyaniline

- supercapacitors (as a nanofiber composites of Graphene/Polyaniline) [54]
- batteries (PANI used as an anode) [55]
- biosensors (PANI as an electrochemical biosensor for detecting biological compounds) [8]
- corrosion (used for corrosion prevention) [56].

1.6 Electrochromism

Electrochromism is the phenomenon of reversibly changing color displayed by a material upon reduction or oxidation, when placed in an electric field. In the later 1960s, it was found that transition metal oxides have the capability of reversibly changing colors[57]. Since PANI shows excellent color transition, it is an excellent electrochromic material, as it transitions from yellow-green to dark blue. An electrochromic device (ECD) can be created by sandwiching two

electrodes (polymer electrodes) together with an electrolyte in between (mostly an acidic medium), and applying a potential across as shown in figure 22. The polymer based ECD can consist of one electrode made of PANI and the other made of poly(3,4-ethylenedioxythiophene)(PEDOT) conducting polymer, or a simple polyaniline /electrolyte/conducting ITO glass plate.

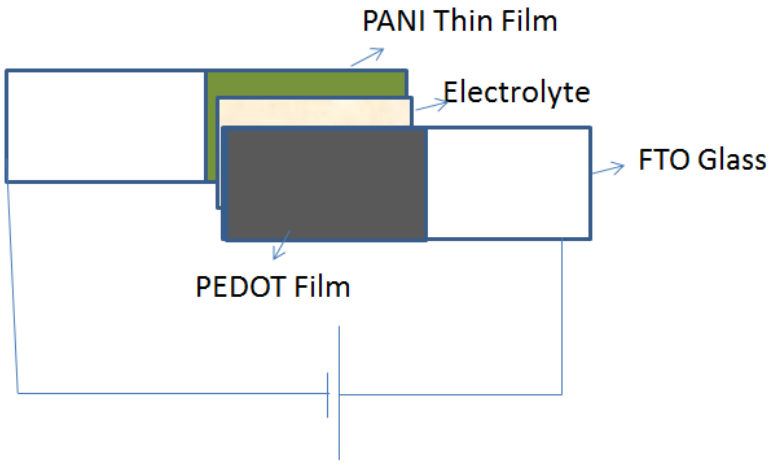

Figure 22 Electrochromic device consisting of PANI/PEDOT.

ECDs have many applications. It can be used as a reflective electrochromic device by self-darkening to allow better vision for the driver in the night vs. the morning. It can also be used for sunglasses , visors, and energy application in smart building windows.

CHAPTER 2. CHARACTERIZATION AND ELECTROCHEMICAL TOOLS

2.1 Characterization Tools

2.1.1 UV-Spectroscopy

UV spectroscopy is the measurement of the absorption of the beam of light when it passes through a substrate, or it can be a measurement of reflectance, where the beam of light is reflected at the sample's surface. It is used to study many characterization techniques such as absorption, transmission, and reflectivity of various materials; as well as studying the optical and electronic properties of materials. The spectral region of the UV/Vis is in the visible UV and near infrared. The perceived color of the chemical is affected when there is an absorption in the visible range [58]. V530 Jasco Spectrophotomer (figure 23) was used to extract the UV spectrum of the polyaniline films.

Figure 23 UV/Nis spectrophotometer.

2.1.2 FTIR

Fourier transform infrared spectroscopy is a technique used to determine and measure the absorption of light in the infrared spectrum at each wavelength. It can also be used as a quantitative technique to identify unknown materials, and the amount of components in a mixture. The spectrum results in certain absorption peaks, which are frequencies from vibrations of the bonds of the atoms. The size of the peaks provide us the amount of each material present in the substrate [59]. Perkin Elmer Spectrum One FTIR spectrometer was used in both transmission and reflection mode, to understand the doped polyaniline films, dye doped, or composite polyaniline films (figure 24).

Figure 24 FT-IR spectrometer.

2.1.3 SEM

Scanning Electron Microscope (SEM) is the tool used to study the microscopic structure of the different samples. It is the most used electron microscope. The image is obtained by scanning the surface of the sample using a focused electron beam [60]. The most attractive feature of SEM is

its 3-D image, which is due to the large depth of field. The SEM depth of field can reach up to a magnification of 10^4. The Ultra-high Resolution SEM SU-70 Hitachi was used as shown in figure 25.

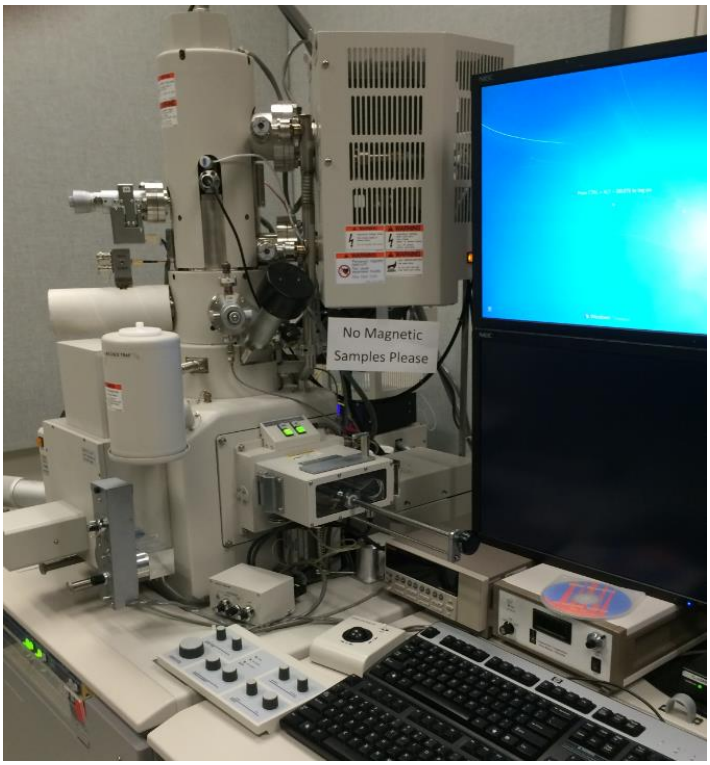

Figure 25 SU70 Hitcha scanning electron microscope instrument.

2.1.4 XRD

X-Ray diffraction is a method used to determine the material's crystal structure. As such, the chemical compounds could be extracted. The instrument used was an x-ray diffractometer with an electromagnetic radiation with a short wavelength. XRD works by measuring the diffraction intensity by varying the incident angle of the beam [60]. Analytical X'Pert XRD instrument was used for all the samples used in this thesis as shown in figure 26.

Figure 26 XRD instrument- Analytical X'Pert.

2.1.5 I-V Characteristics

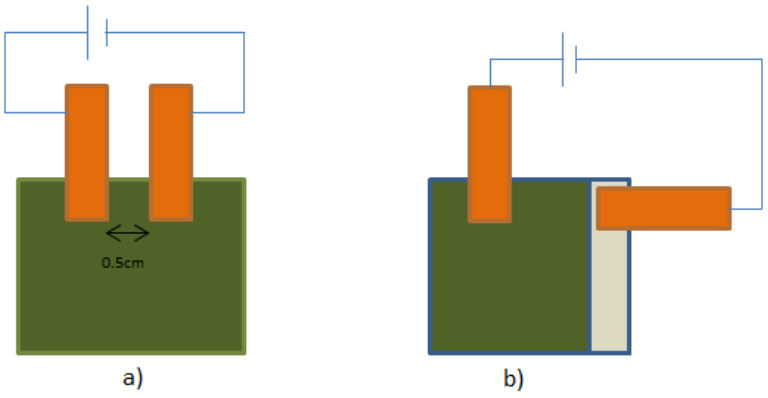

Figure 27 Experimental set up for extracting polyaniline's electrical properties.

The electric properties of polyaniline were extracted by studying the linear potential method using the Voltamaster software. As such, a current density vs. voltage plot was obtained. Two

setups were used using a two point electrode: a lateral connection and an across connection. Figure 27 shows the two different type of setups. Figure 27a) consists of a uniform polyaniline film where two copper foils were taped at a distance of 0.5 cm of each other. Figure 27b) consists of one copper tape on PANI, and the other tape was on the FTO (without PANI).

2.2 Electrochemical Tools

2.2.1 Cyclic Voltammetry

Cyclic voltammetry (CV) is a potentiodynamic technique, where the working electrode is ramped linearly and is inverted when a specific potential is reached. The cyclic voltammetry is a function of time. CV can be used to study a various range of electrochemical reactions. The three point electrode method was used, with Ag/AgCl as a reference, FTO as working, and platinum as counter electrode. The current flow through the working electrode was measured, and the potential is acquired by computing the current against the reference electrode. On the other hand, the counter electrode is used to finalize the electrical circuit for the current flow [61, 62].

Furthermore, Randles- Sevcik equation was used to calculate the diffusion coefficient using the following equation [63]:

$$i_p = 268{,}600 n^{\frac{3}{2}} A D^{\frac{1}{2}} C v^{1/2}$$

i_p= maximum current in amps

n= number of electrons transferred in the redox event

A= electrode area in cm^2

F= the Faraday constant in C mol^{-1}

D= diffusion coefficient in cm^2/s

C= concentration in mol/cm^3

v = scan rate in V/s.

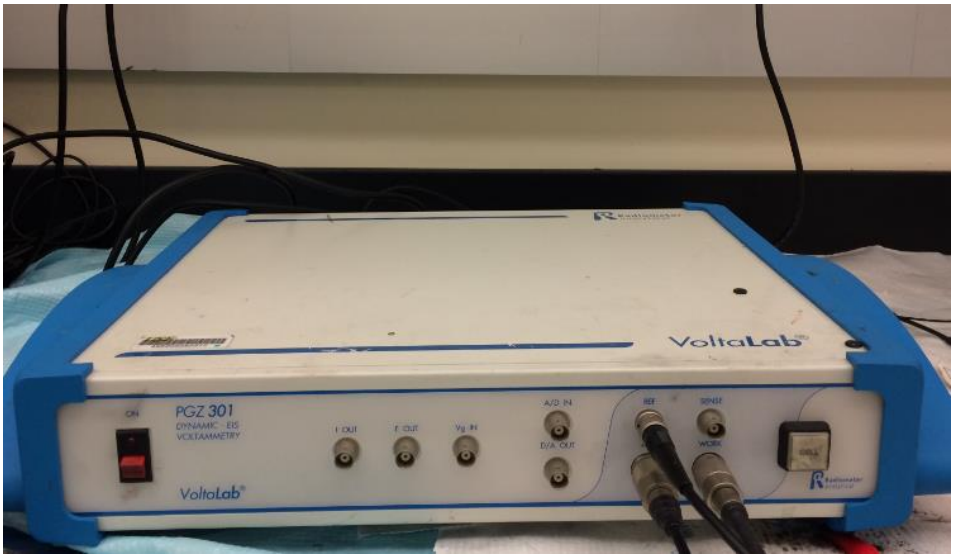

Figure 28 VoltaLab instrument for CV and CA measurements.

VoltaLab PGZ301 instrument was used to study the cyclic voltammetry as shown in figure 28.

2.2.2 Chronoamperometry

This electrochemical technique provides the current from a faradic process, which occurs at the electrode as a function of time. The signal is given as a stepped pulse as the potential at the working electrode is given at a constant value E_0, then increases instantaneously at a new value E_1 [62]. Again, VoltaLab PGZ301 was used to study the chronoamperometry (CA).

2.2.3 Electrochemical Impedance Spectroscopy

Electrochemical impedance spectroscopy (EIS) is a tool used as a characterization technique of the dynamics of an electrochemical process [64]. It has many applications in corrosion [65], plating [66], batteries [67], etc. It works by studying the response of the system as a function of

the frequency [68]. For the Electrochemical Impedance Test, Gamry Reference 600 was used (figure 29).

Figure 29 Gamry instrument for electrochemical impedance spectroscopy.

CHAPTER 3. SYNTHESIS AND CHARACTERIZATION OF PANI

3.1 Synthesis

The film used was deposited using the process of self-assembly. Three films were made: polyaniline with 1 layer, 2 layers, and 3 layers. For multiple layers, the film was rinsed with HCl and dipped again to go through a self-assembled film formation. Self-assembly is a process defined as the spontaneous organization of molecular units without external direction, which creates a self-assembly monolayer (SAM). These molecules adsorbs on the substrate spontaneously to form a thin layer [69]. Throughout my research, many deposition techniques have been used (solution casting, vacuum deposition, etc.); however, in-situ self-assembly has provided me with the best PANI film displaying a uniform layer. Before depositing the PANI film, the FTO glass is dipped in a poly(styrene sulfonate)(PSS) for 24h. PSS is used to enhance the polymerization of PANI, due to its negative charge. To oxidize this polymer, we mix aniline with APS in an acidic aqueous medium (HCl). A mixture of 0.2 M of with 0.25 M of APS in 0.2 M of HCl is dissolved in 50 mL of DI water at room temperature [45]. Figure 30 shows the oxidation process of the aniline in a medium containing HCl and APS, which results in the formation of emeraldine. When all components are dissolved, a glass support with an area of 6 cm^2 is inserted into the mixture. The non-conductive side of the glass was taped allowing the film to only form in the conductive side of the glass. There is a short induction period, where the mixture is colorless and the temperature stays the same. When the oligoaniline radicals are created, the mixture turns into a dark blue color. These oligomers start adsorbing themselves at the surface in contact with the aqueous mix.

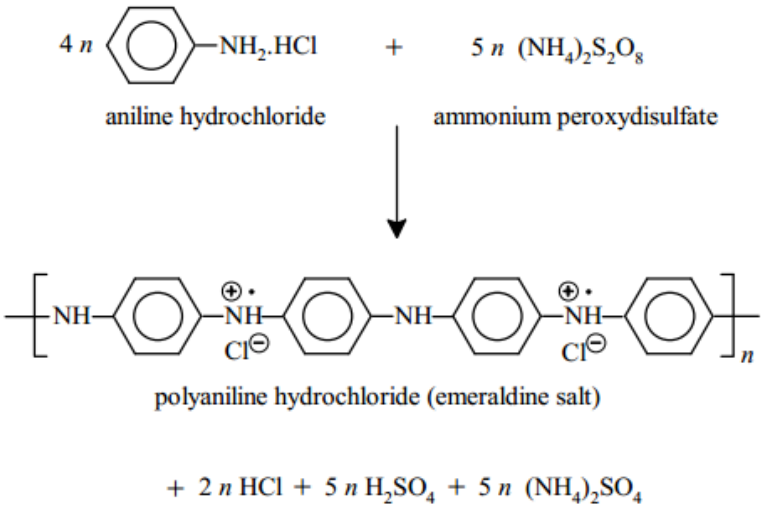

Figure 30 Oxidation of aniline in a medium containing HCl and ammonium peroxidisulfate. Reproduced with permission [48]

This initiates the formation of the first PANI chain, which produces the nucleus of the next film. This is known as the polymerization of aniline. The temperature is at its maximum when the mixture turns into green emeraldine, which is known as the emeraldine salt. The film is then spread on the substrate to form an emeraldine form of PANI [70]. Figure 31 shows the schematic of the PANI thin film deposited on the FTO glass substrate. After polymerization, the film is removed from the solution, rinsed with HCl, and dried with N_2.

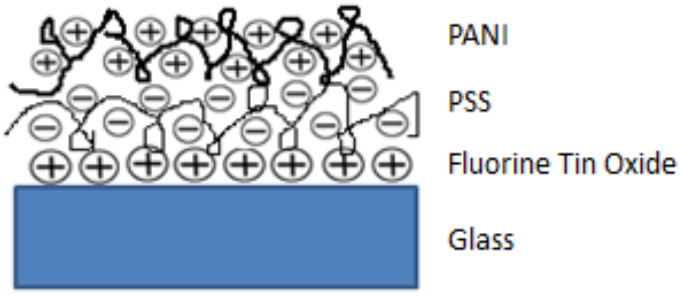

Figure 31 Schematic of the film deposition of in-situ self-assembly of polyaniline films.

3.2 Characterization

3.2.1 UV Spectroscopy

Figure 32 shows the UV spectroscopy of different layers of PANI. The graph displays two maxima located at wavelength at approximately 330 nm and 768 nm. The absorbance for each film has been summarized in table 3. The thickness was extracted using the following equation A(peak)*(λ/2). The peak at around 336 nm is due to π-π* transition, and wide peak at around 820 nm is due to the presence of the dopant. There is an increase in the absorption magnitude as the number of monolayers increases.

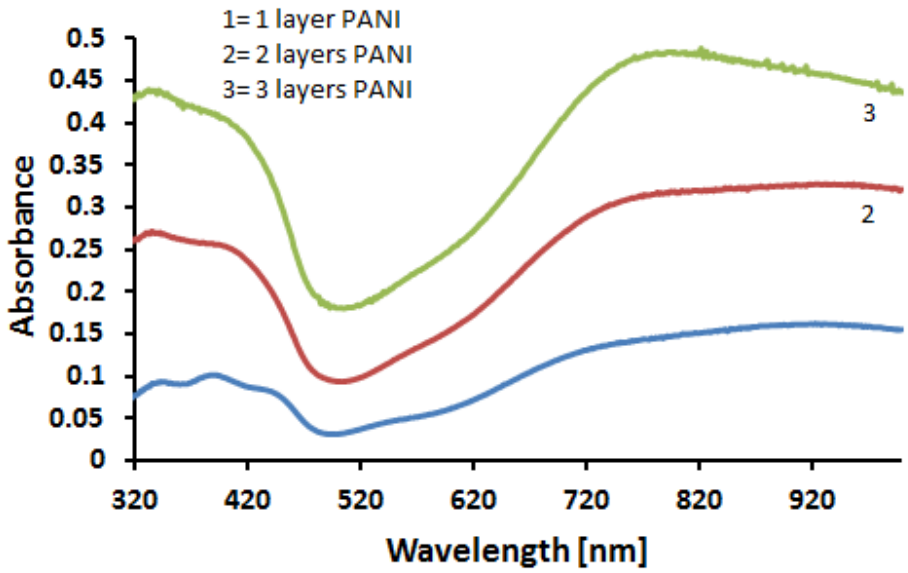

Figure 32 UV spectra of different layers of PANI.

Table 3 Calculation of PANI thickness for different layers.

	λ(nm)	**λ/2(nm)**	**A(λ)**	**d in nm**
1 layer	403	201.5	0.1	20.15
2 layers	336	168	0.27	45.36
3 layers	336	168	0.4375	73.5

3.2.2 FTIR

Figure 33 shows the FTIR spectra of different thicknesses of polyaniline films. The small peak at 1340 cm^{-1} is due to the dopant present while the film is synthesized using the self-assembled technique.

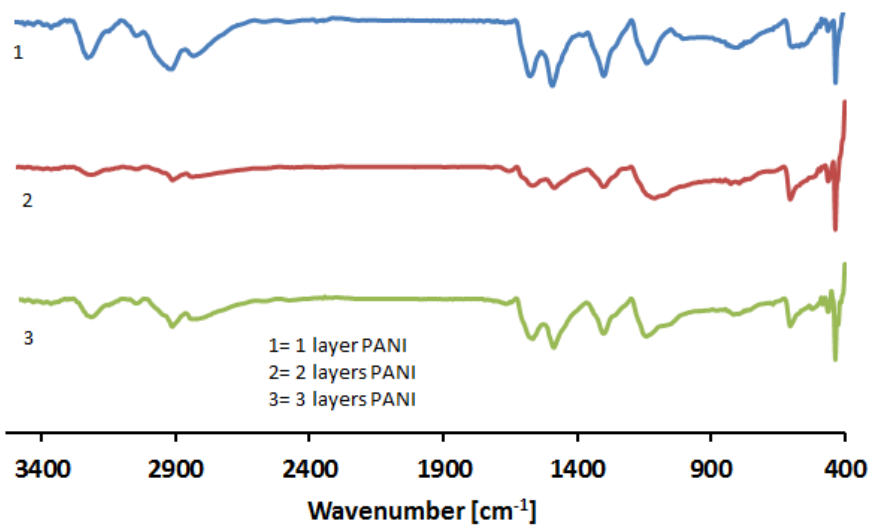

Figure 33 FTIR spectrum of different thickness polyaniline thin films.

Table 4 shows the characteristic peaks of different layers of PANI thin film.

Table 4 Characteristic peaks of different layers of PANI thin film.

cm^{-1}	**N-H stretching**	**C-H stretching**	**C=C stretching aromatic nuclei**	**C=C aromatic compound**	**C-N stretching**	**C-H bending vibrations**
1 Layer PANI	3224	2916	1577	1491	1307	1151
2 Layer PANI	3219	2912	1574	1488	1304	1137
3 Layer PANI	3232	2926	1582	1501	1297	1145

3.2.3 Morphology of PANI Films

Figure 34 shows SEM images of different layers of PANI deposited on FTO glass. The film containing one layer (figure 34a) has a compact PANI layer deposited on the electrode's surface. As the thickness increases, a fiber-like PANI is formed around the particles (figure 34b). In figure 34c), the porous fiber PANI has covered most of the thin films' surface. This can be explained by having polyaniline and its oligomers simultaneaously deposited on the substrate.

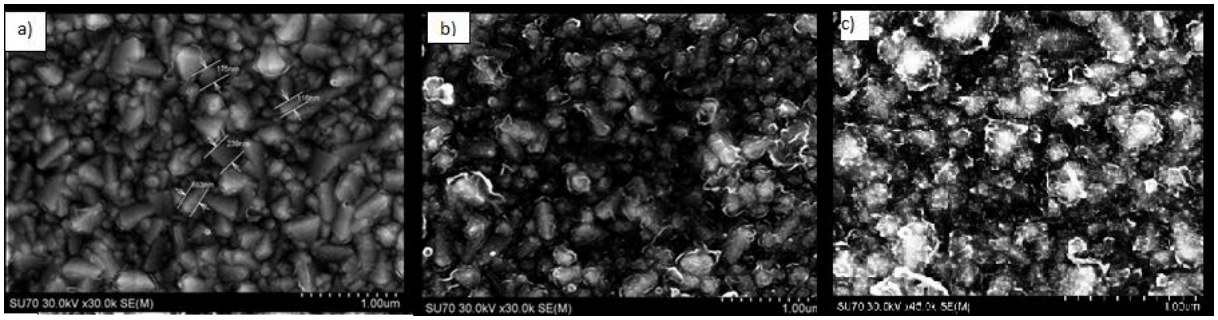

Figure 34 SEM images of different layers PANI films. a)1 layer PANI b)2 layers PANI c)3 layers PANI.

3.2.4 XRD

Figure 35 shows the XRD pattern for the PANI films with different thicknesses. The peaks occur at 2θ =27º, 38º, 52º, 62º, and 66º, which corresponds to the crystallinity of FTO. The XRD pattern does not, however, provide any trace for the PANI films [71].

Since, the peaks did not show on FTO glass. Polyaniline was deposited on silicon wafers. No peaks were present for 1 and 2 layers. The reason for the absent peaks is due to the amorphous behavior the polymer is exhibiting, which is in accordance with literature [72].

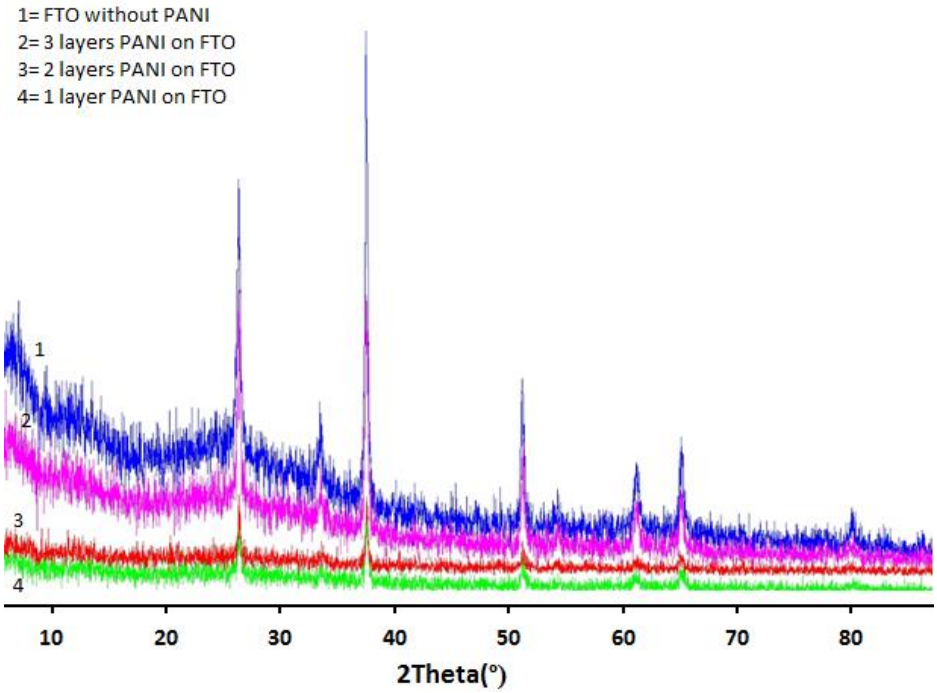

Figure 35 XRD of different layers PANI thin films on FTO.

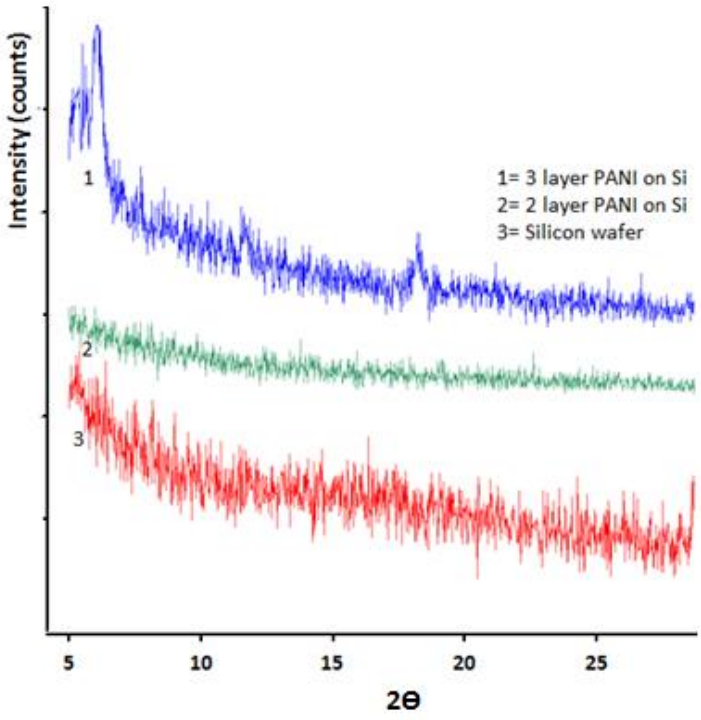

Figure 36 XRD of different layers PANI thin films on silicon.

However, figure 36 shows the XRD peaks present for 3 layers PANI film, which is due to the polycrystalline structure of the thicker thin film. From literature [73], crystalline silicon exhibits three peaks at around 2θ=28.1°, 47.4°, and 56.2°. The peaks of silicon are narrower than the one exhibited by PANI/Si, hence it can be concluded that the particle size decreases when PANI is deposited on the Silicon. From XRD measurements done in figure 36, there are three peaks which corresponds to the to the PANI thin film at 2θ= 12.8°, and 18.2°. Moreover, the film deposition of PANI did not change the crystallinity of the silicon wafer. Note that similar method of in-situ self-assembly deposition was used to coat the silicon wafers.

3.2.5 I-V Characteristics

For the lateral set up, all samples studied exhibited Ohmic behaviors. Figure 37 shows the results of the current density vs. voltage for 1 layer polyaniline in the "across" set up. The film represents a nearly ohmic behavior for higher scan rate. However, for lower scan rates, there are some disturbances seen during the higher voltages in both the forward and reverse bias.

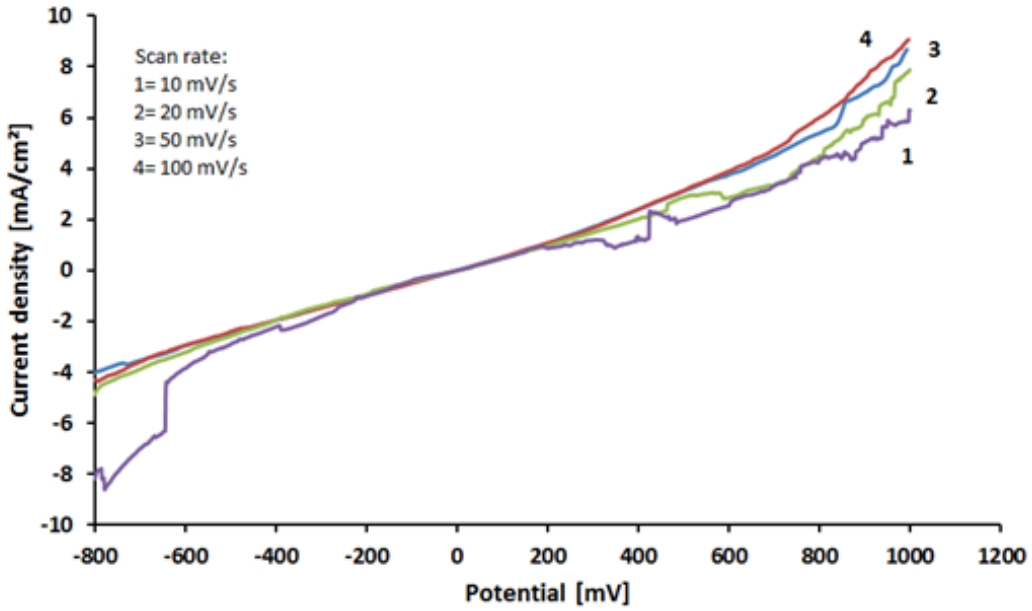

Figure 37 Current density vs. potential for 1 layer PANI/across.

Figure 38 represents the current density vs. potential for 1 layer PANI in the lateral position. The film has an Ohmic behavior for the entire scan rate due to asymmetric charge transfer from the polyaniline contact with the copper metal.

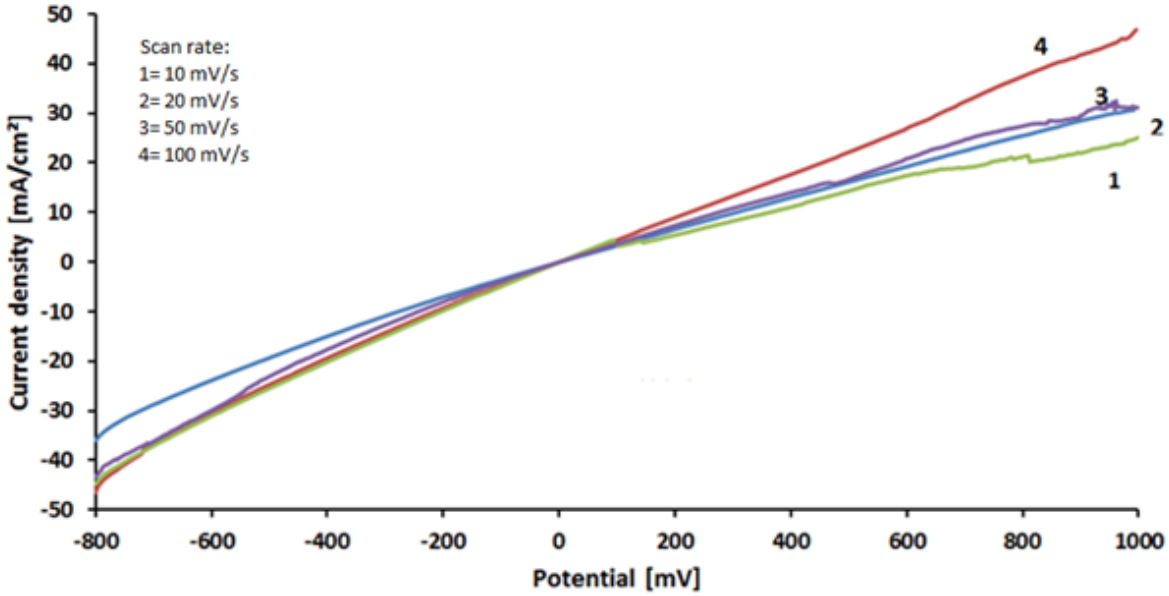

Figure 38 Current density vs. potential for 1 layer PANI/lateral.

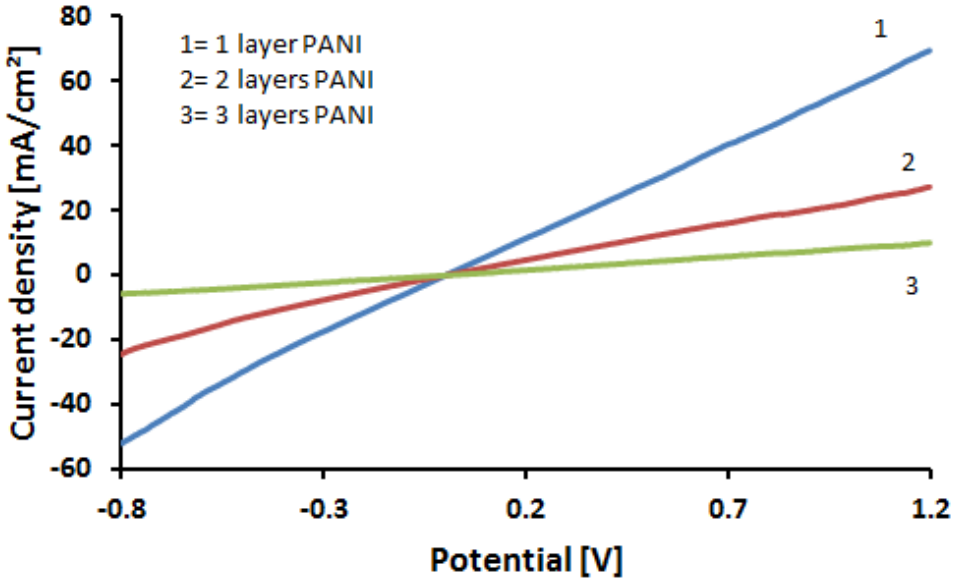

Figure 39 Comparison of different thicknesses of PANI/lateral at 50 mV/s.

Figure 39 compares the current density vs. potential for different PANI thicknesses at room temperature. The conductivity of the thin film increases with increasing film thickness. FTO creates an Ohmic behavior to PANI, which corresponds to a P-type semiconductor.

The ideality factor (n) was calculated by plotting ln(I) vs. voltage, and the slope is equal to q/nkT where:

k (Boltzmann constant)= $1.3806488*10^{-23}$ JK^{-1}

q (electric charge)= $1.6021765*10^{-19}$ C

T= room temperature

solving for the ideality factor, n

Table 5 The ideality factor for different PANI thicknesses.

1 layer PANI	22.15233009
2 layer PANI	30.17832735
3 layer PANI	8.483822155

CHAPTER 4. DYE INCORPORATION

4.1 Introduction to Dye Incorporation

In order to expand the color spectrum of these thin films, two dyes were incorporated: Rhodamine B and Prussian Blue. Rhodamine B is a red fluorescent dye that is soluble in water. It is mainly used to trace water for rate flow determination [74]. Recently, it has been used as a main component for the dye-sensitized solar cell based of polyaniline electrodes [75]. Rhodamine B has the molecular formula of $C_{28}H_{31}ClN_2O_3$[76].

Prussian Blue, on the other hand, is a dark blue dye of the hexacyanoferrate family. Its molecular formula is $C_{18}Fe_7N_{18}$. Its main application is used as an antidote for metal poisoning in the medical field [77]. As such, it has been used with polyaniline as an amperometric biosensor for detection of uric acid [78].

4.2 Synthesis- Electrochemical Deposition

Electrochemical deposition was used to make a polyaniline thin film with Rhodamine B dye. The electrodeposition was carried in a three point-electrode cell, which consisted of a fluorine doped tin oxide (FTO) coated glass slide, with a surface resistivity of 10 Ω/sq. as a working electrode. The reference electrode consisted of an Ag/AgCl electrode, and the counter electrode was a platinum wire. The area of the working electrode was 4 cm^2. The resulting film was achieved by a chronoamperometry synthesis of 1M HCl+0.2 M PANI+0.00125 M Rhodamine B dye electrolyte.

For PB, the deposition was obtained by cycling the potential from 0.6 V to 0.2 V at 100mV/sec [79]. The 2 layer PANI thin film was dipped in a three point electrode similar to the previous electrodeposition in an electrolyte solution consisting of 0.25 M $KHSO_4$, 0.0005M of $K_3Fe(CN_6)_6$, and 0.005 M $Fe_2(SO_4)_3$. Both dye depositions were done using Voltamaster software.

4.3 Characterization

4.3.1 UV Spectroscopy

Figure 40 below corresponds to the UV spectra for dye incorporated thin films. The PB/PANI and RhB/PANI do not exhibit the same peak location, since both utilizes different deposition techniques and utilizes different dyes. Again, using the peak positions, the film thickness was extracted. Table 6 summarizes all the results.

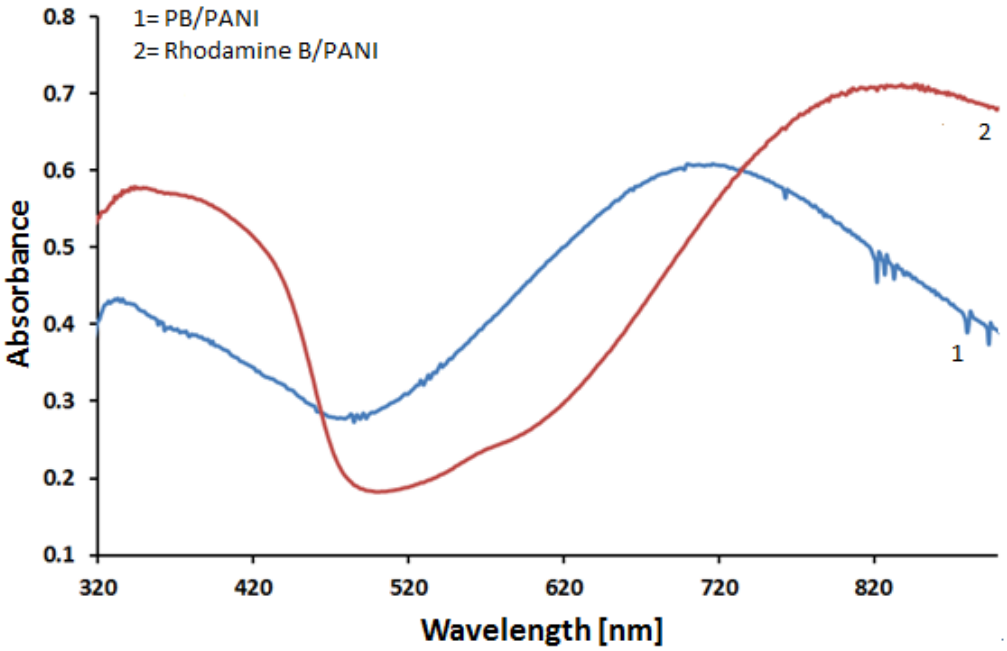

Figure 40 UV spectra for dye incorporated PANI thin films.

Table 6 Calculation of film thickness from UV-Spectra.

	λ	λ/2	A(λ)	d(nm)
PB/PANI	329	164.5	0.43	70.735
Rhodamine B	356	178	0.58	103.24

4.3.2 FTIR

Figure 41 below shows the FTIR spectra of dye incorporated films. Table 7 summarizes all characteristic peaks. There is a characteristic peak in the PB at 2050 cm^{-1}, which corresponds to the Fe-CN stretching mode in the cyanometallate lattice [80].

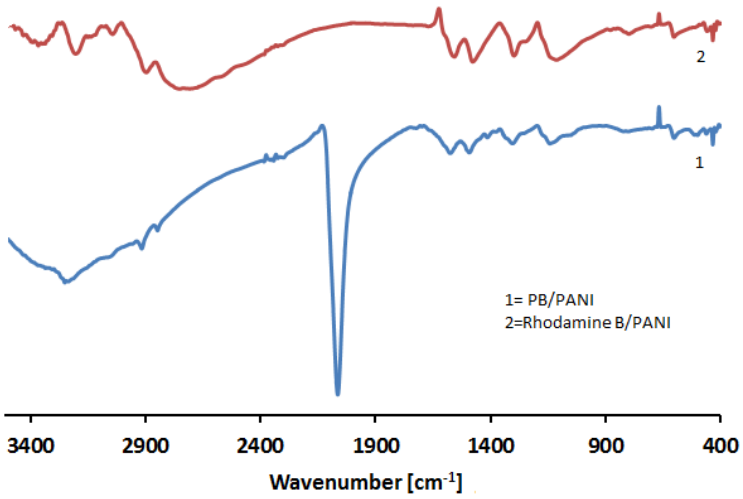

Figure 41 FTIR results of dye incorporated thin films.

Table 7 Characteristic peaks of dye incorporated films.

Cm^{-1}	**N-H streching**	**C-H stretching**	**C=C stretching aromatic nuclei**	**C=N in aromatic compound**	**C-N stretching**	**C-H bending vibrations**
PB/PANI	3247	2915	1580	1499	1308	1151
RhB/PANI	3222	3045	1565	1484	1301	1116

4.3.3 SEM

In figure 42a, new noticeable particles were on top of the PANI thin film; this can be explained by PB deposited on the already pre-existing PANI layer. On the other side, figure 42b, porous PANI fibers were observed, which is due to the high potential range used to deposit PANI on FTO glass.

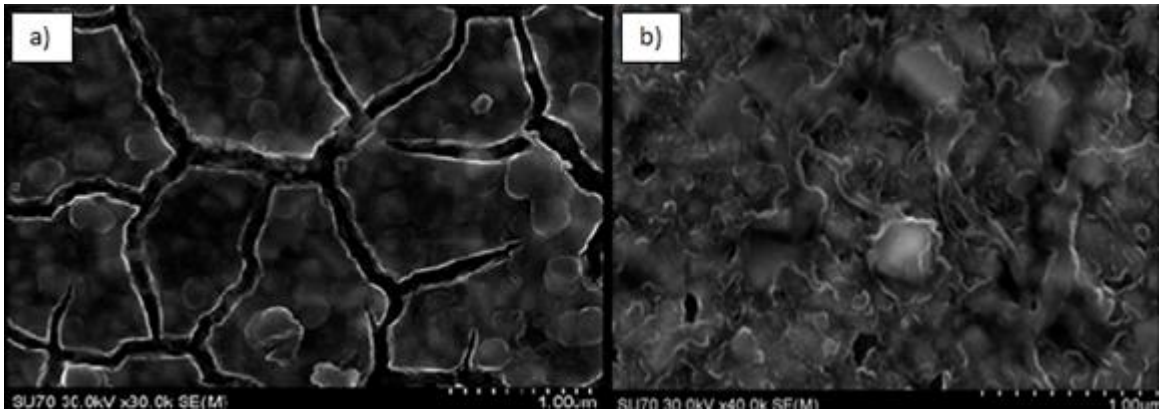

Figure 42 SEM images of dye incorporated PANI films. a) PB/PANI B) RhB/PANI.

4.3.4 XRD

No trace of PANI, Prussian Blue, or Rhodamine show on the XRD results in figure 43. The peaks occur at the same position as the different layers of PANI, and correspond to the polycrystallinity of the FTO glass substrate.

As the peaks were not present in the previous method, the dye incorporated films were deposited on silicon. The XRD measurements are shown in figure 44. No peaks of RB/PANI were observed since it exhibits an amorphous nature. However, a peak at $2\theta=26^0$ is noticed on the PB/PANI, which corresponds to the PB nanoparticle.

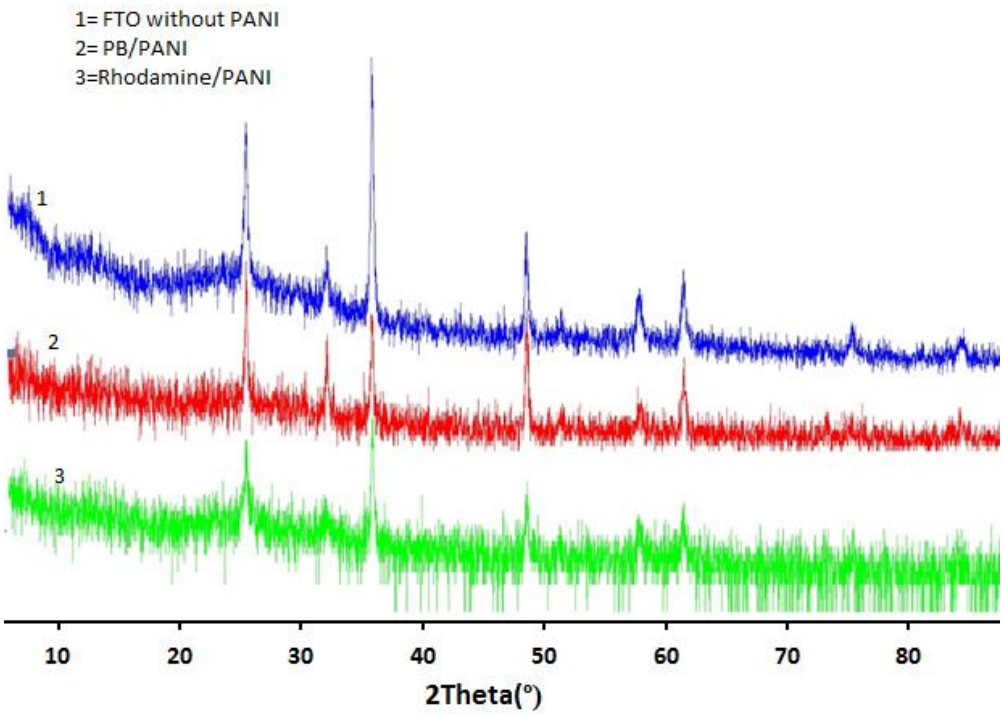

Figure 43 XRD of dye incorporated thin films on FTO.

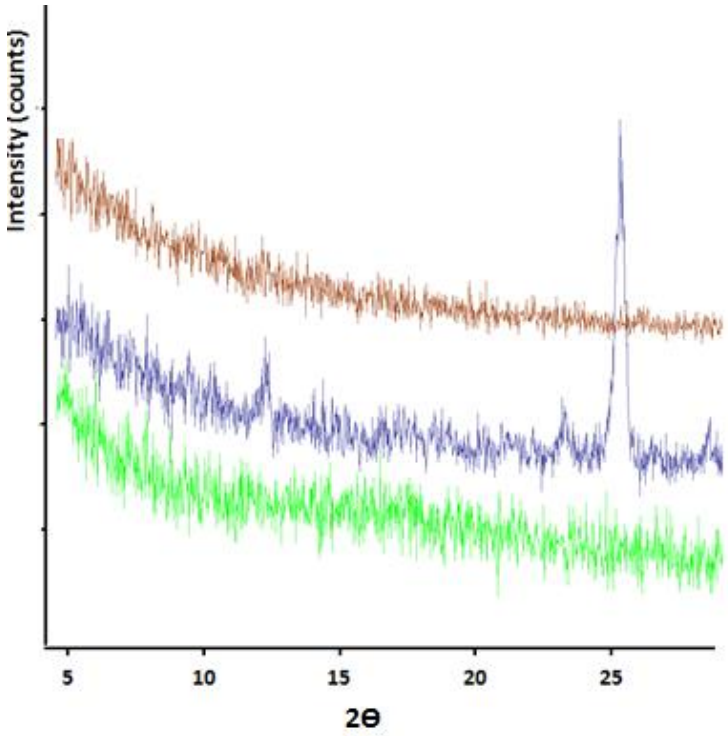

Figure 44 XRD of dye incorporated polyaniline thin films on silicon.

4.3.5 Electrical Properties

Figure 45 shows the current density vs. voltage at a scan rate of 10 mV/s for the dye incorporated thin films. The I-V characteristics of the film exhibit the behavior a normal diode. We can see that the avalanche breakdown occurs at -500mV to -1000mV for both 1 and 2. The knee point in the forward bias can be seen at around 1000mV for both 1 and 2.

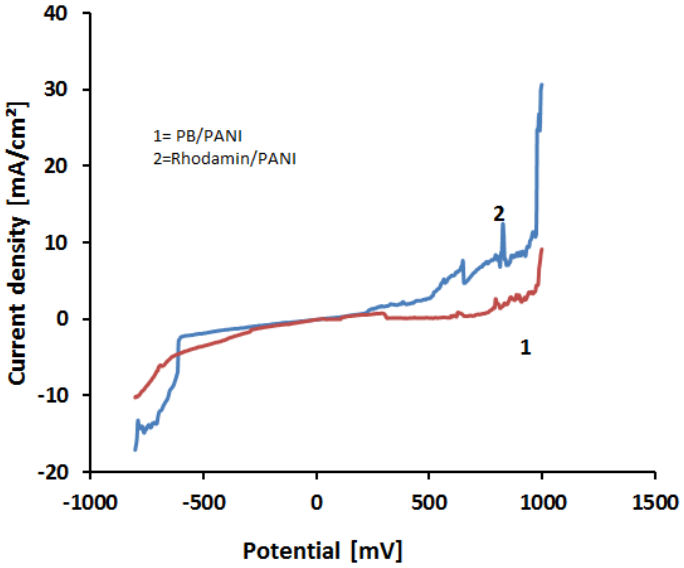

Figure 45 Current density vs. potential for dye incorporated films/across.

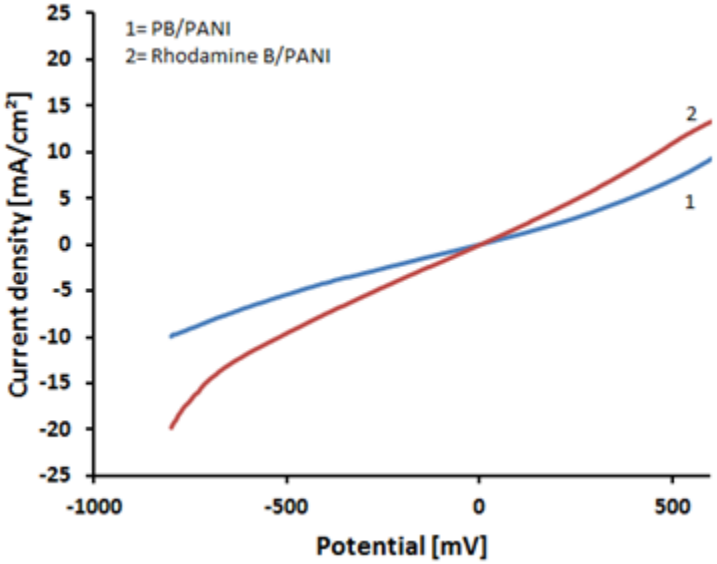

Figure 46 Current density vs. potential for dye incorporated films/lateral.

Figure 46 represents the current density vs. the potential for the dye incorporated thin films in the lateral set-up. Same behavior is displayed here similar to the plain PANI films. The film represents a nearly Ohmic behavior due to asymmetric charge transfer in the polyaniline contact with the copper metal.

Using the same method previously discussed in the plain PANI films to extract the ideality factor, the following values were obtained.

Table 8 The ideality factor for dye incorporated PANI films.

PB/PANI	12.19
RhB/PANI	16.411

CHAPTER 5. ELECTROCHEMICAL APPLICATION

5.1 Experimental Set-up

To study the electrochromic properties, a three point-electrode cell, with an Ag/AgCl reference electrode, and a platinum wire counter electrode. The work electrode consisted of PANI thin films and dye incorporated PANI films as shown in figure 47.

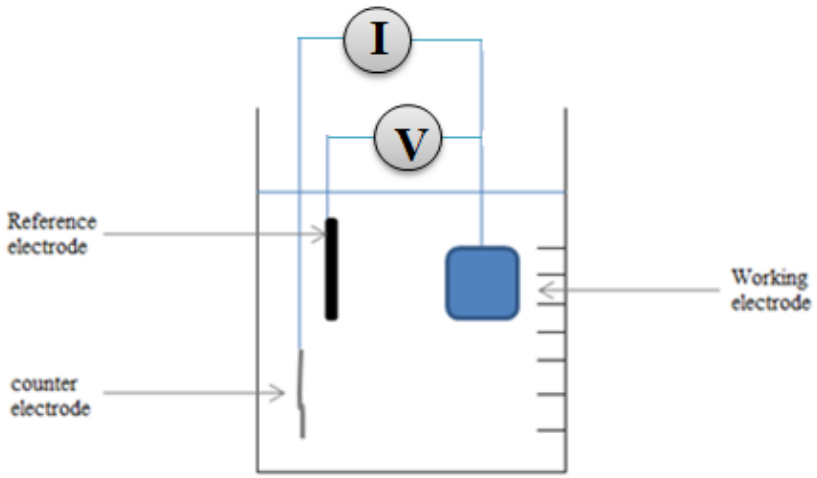

Figure 47 Experimental set up to study the electrochemical properties of thin films.

The electrochemical studies were carried in different acids: 1M lithium perchlorate, 1 M HCl, and 1M sulfuric acids. Furthermore, electrochemical methods were carried using different electrolytic consistencies: gelatin based electrolyte and polyvinyl alcohol based electrolyte. The software used was the Voltamaster as described in the previous chapter.

5.2 Electrochemical Methods

5.2.1 Cyclic Voltammetry

The cyclic voltammograms of the PANI films were recorded at 1 M HCl in three different states: liquid and semisolid (Gelatin based electrolyte and PVA based electrolyte) for different PANI films. Figure 48 shows cyclic voltammograms of 1 layer PANI in 1M liquid HCl from 10 mV/s to 100 mV/s. The redox pairs are assigned as AA', BB', and CC'. The increase of the sweep rate does influence the position of all the potential peaks. The anodic peaks shift towards a high potential; on the other side, cathodic peaks shift towards a lower potential. Also, at a sweep rate of 10mV/s and 20 mV/s, the third reduction peak A' is not noticeable. As the sweep rate increases, A' distinguishly gets noticed. Peak A corresponds to the oxidation change of neutral PANI, and peak C to the oxidation from emeraldine to pernigraniline. For peak B, it can be explained by the degradation of PANI due to soluble species (benzoquinone and hydroquinone) [81]. One layer PANI shows really good electrochemical reversibility.

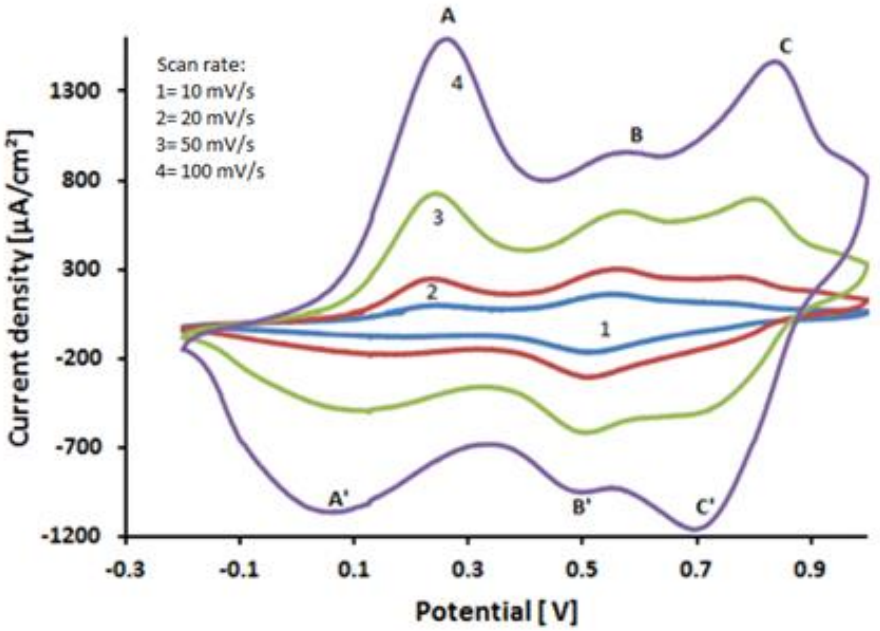

Figure 48 Cyclic voltammetry for 1 layer PANI in 1 M liquid HCl.

5.2.1.1 Comparison to Different Acids

Figure 49 shows the cyclic voltammograms of 1 layer PANI in 0.1 M lithium perchlorate electrolyte. Both of the anodic and cathodic peaks are absent. Figure 50 shows the cyclic voltammograms for 1 layer PANI in 1 M sulfuric acid. Three redox peaks are noticeable for 100 mV/s, 50 mV/s, and 20 mV/s. The voltammetry exhibits the same behavior as the one observed in 1 M HCl. The increase of the sweep rate does influence the position of all the potential peaks. The anodic peaks shifts towards a high potential; on the other side, cathodic peaks shifts towards lower potentials.

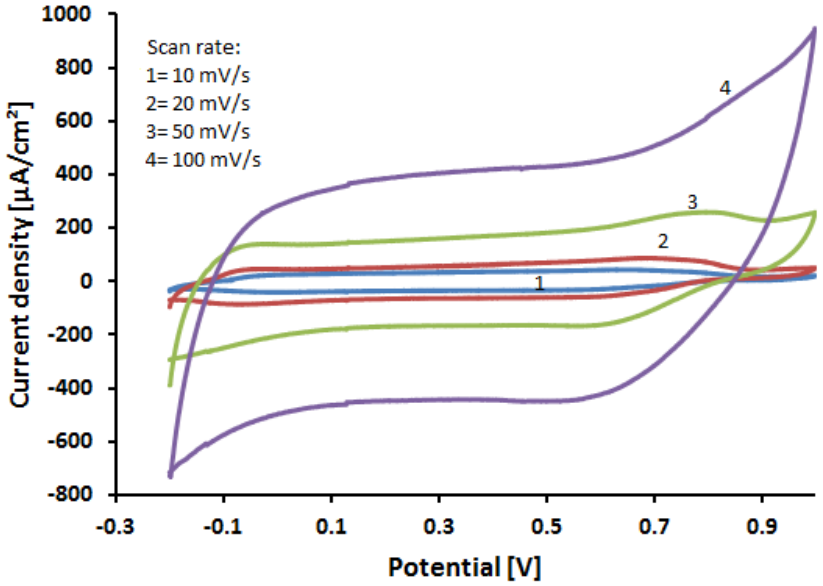

Figure 49 Cyclic voltammetry for 1 layer PANI in 0.1 M lithium perchlorate.

Furthermore, HCl compared to lithium perchlorate and sulfuric acid shows a larger potential difference in the redox peaks, which gives a higher working potential. There is also perfect symmetry displayed by HCl, which shows a better cyclic reversibility.

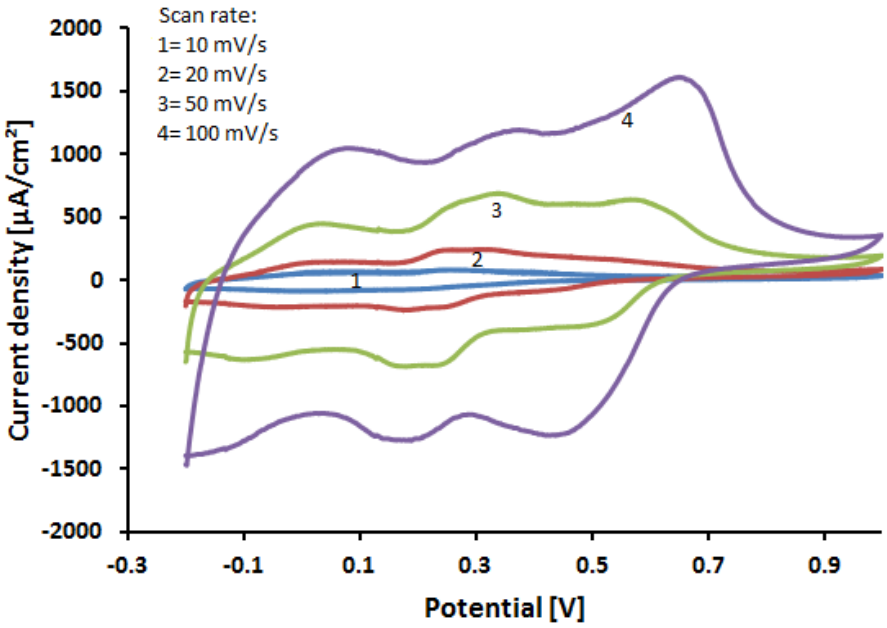

Figure 50 Cyclic voltammetry for 1 layer PANI in 1M sulfuric acid.

5.2.1.2 Comparison to Different Electrolyte Consistencies

Both figure 51 and 52 exhibit three redox peaks similar to the liquid 1 M HCl. However, the BB' pair in the PVA and gelatin based is barely noticeable comparing to the one exhibited by the liquid electrolyte. The PVA is also a viscous gel, which doesn't allow the ion to intercalate with the polyaniline molecules. So, the figure 51 and 52 do not show the complete oxidation and reduction process. The increase of the number of layer also decreases the diffusion of the PVA ion in polyaniline structure. For the anodic peak A and B, both gel and PVA show no increase in potential when the scan rate increases; however peak C, when scan rate increases, the peaks shift towards a greater potential. For the cathodic peaks, Peak C', shows no increase in potential as the scan rate increases. On the other hand for peak A', the peaks shift towards a small potential as the scan rate increases.

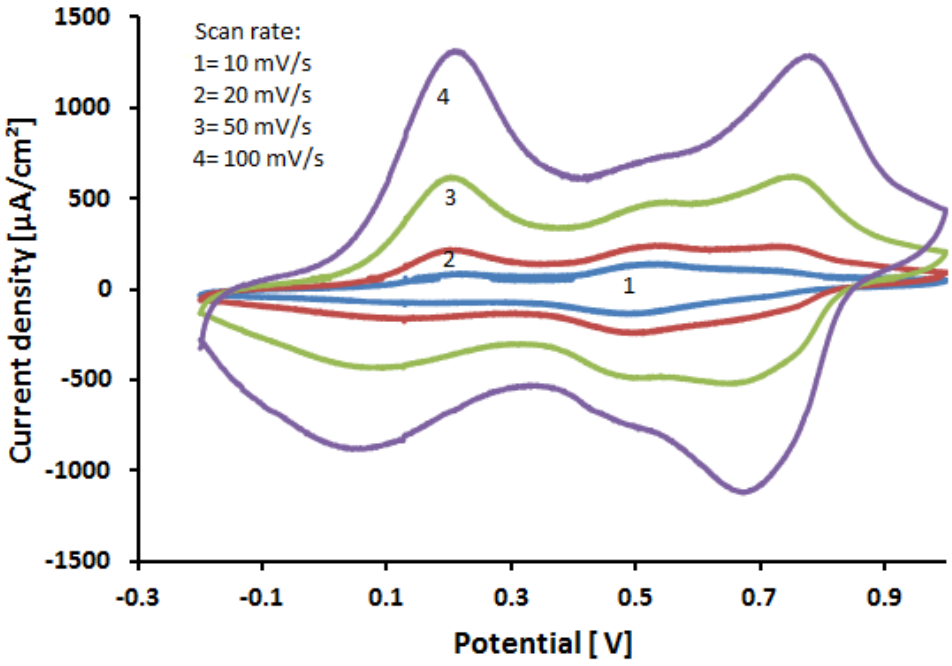

Figure 51 Cyclic voltammetry for 1 layer PANI in 1 M HCl/PVA.

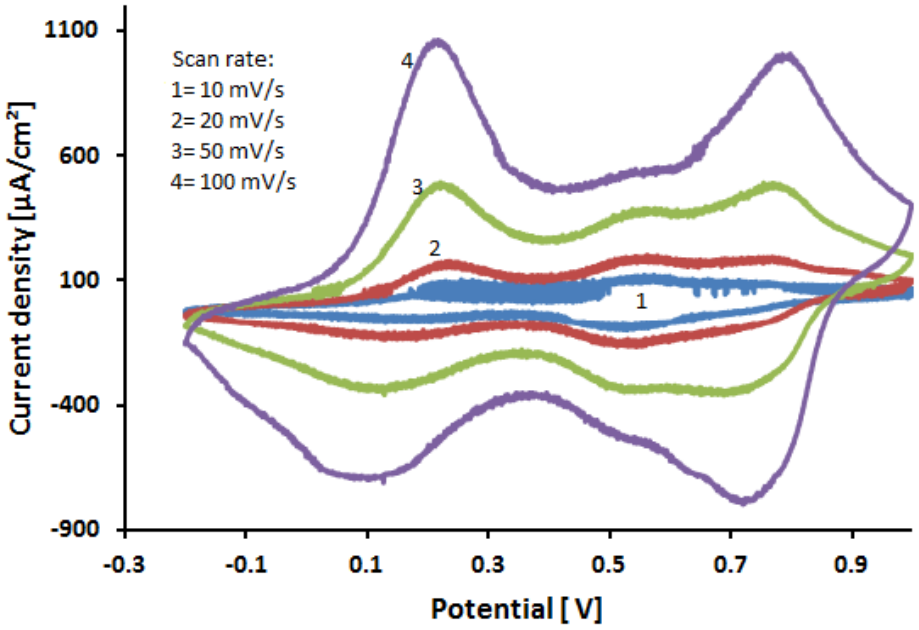

Figure 52 Cyclic voltammetry for 1 layer PANI in 1 M HCl based gelatin.

5.2.1.3 Comparison to Different Thicknesses

In figure 53, for 100 mV/s, only two redox peaks are noticeable. On the other hand, for the other scan rates, three redox peaks can be noticed. As the scan rate increases, the potential shifts towards a greater potential.

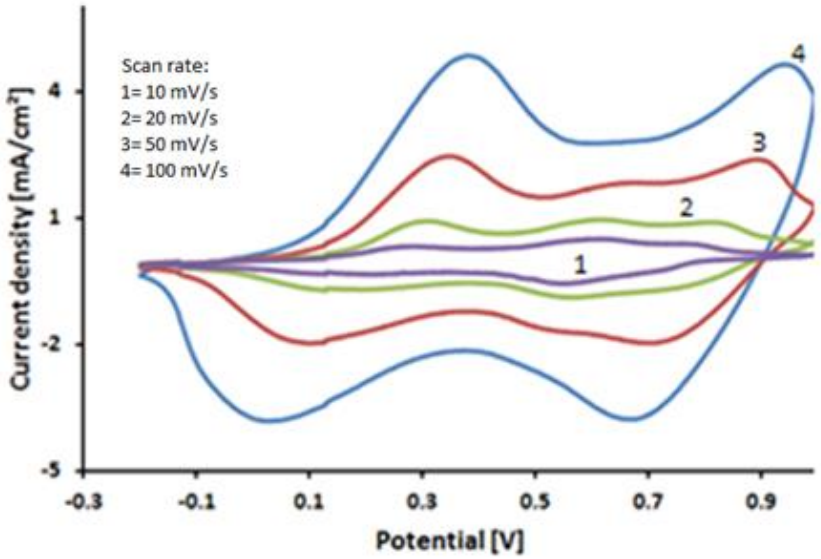

Figure 53 Cyclic voltammetry for 2 layers PANI in 1 M liquid HCl.

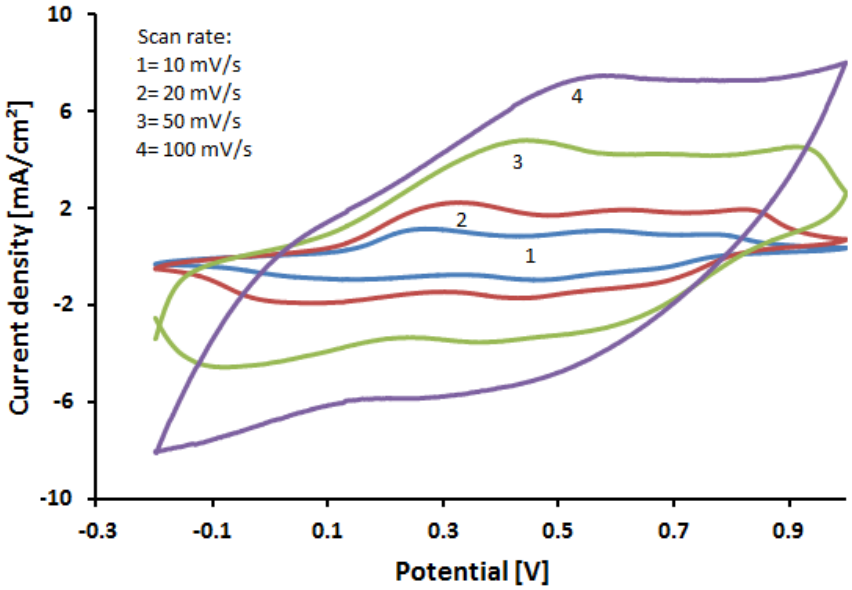

Figure 54 Cyclic voltammetry for 3 layers PANI in 1 M liquid HCl.

As the thickness increases, the peaks become more and more unnoticed (figure 54). As the scan rate decreases more peaks become noticeable, and the potential shifts towards a smaller potential.

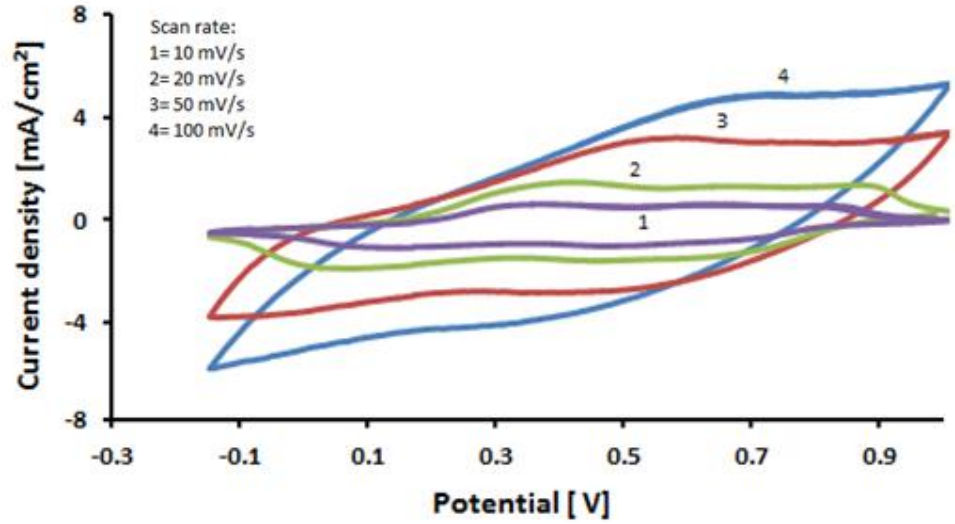

Figure 55 Cyclic voltammetry for 4 layers PANI in 1M liquid HCl.

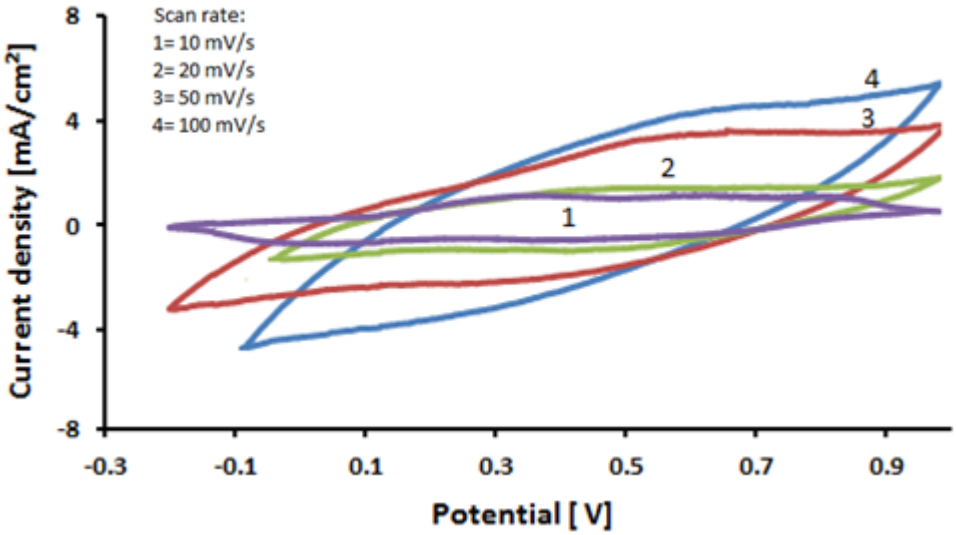

Figure 56 Cyclic voltammetry for 5 layers PANI in 1M liquid HCl.

To further understand the electrochemical properties of different PANI thicknesses, a 4 layer PANI and a 5 layer PANI were studied as shown in figure 55 and 56 consecutively. The range of

the current density is compressed as the film thickness grows, and also, the peaks are less and less noticeable with an increasing scan rate. The electrochromicity of the films is poor comparing to the thinner PANI films. Moreover, the same is noticed here with the previous PANI films, with increasing scan rate the potential is increasing. The thicker film does not allow the faster intercalation/deintercalation of acid ions with polyaniline films.

5.2.1.4 Comparison to Dye Incorporation

For Rhodamine B/PANI, two redox peaks are noticeable for the scan rate of 100 mV/s as shown in figure 57; however, as the scan rate decreases, a third redox peak appears.

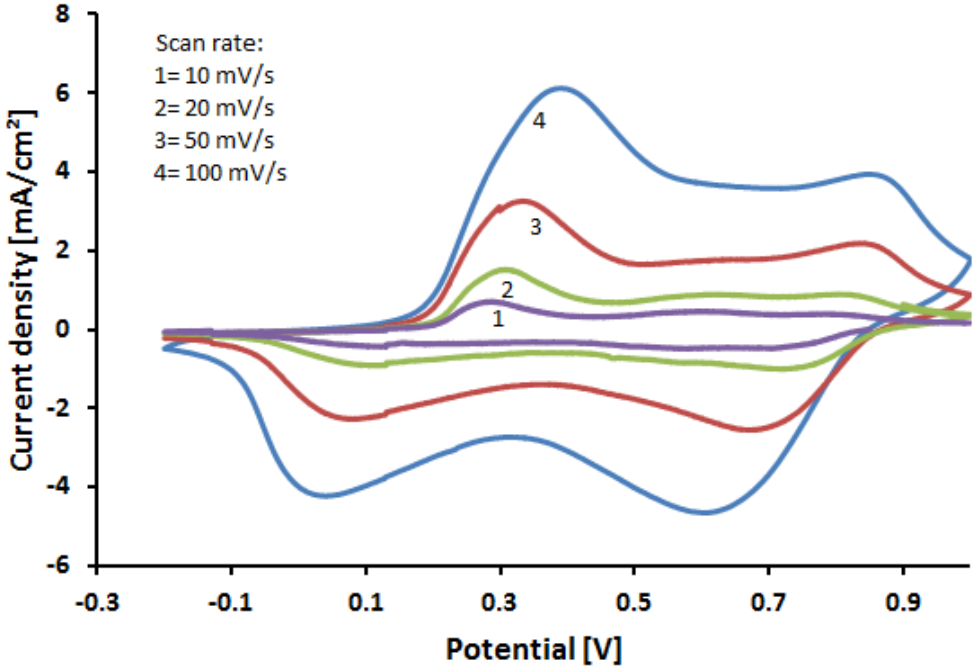

Figure 57 Cyclic voltammetry for PANI with rhodamine B dye in 1 M HCl.

The same phenomenon as the thicker PANI films happens here for PB/PANI (figure 58): the thickness of the film increased, hence the number of peaks displayed are decreasing and are barely noticeable comparing the PANI with one layer.

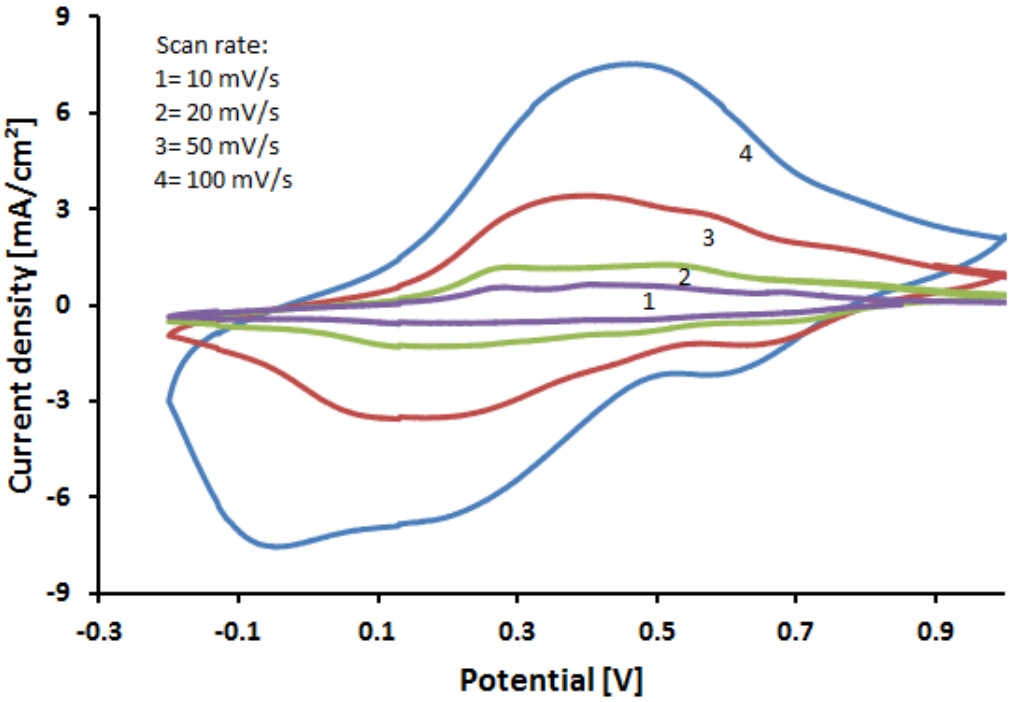

Figure 58 Cyclic voltammetry for PANI with prussian blue dye in 1M HCl.

Table 9 shows the values obtained for the diffusion coefficient calculated using the equation 63 described in Chapter 2 for the different PANI thicknesses.

Table 9 Calculation of diffusion coefficient from the cyclic voltammetry.

n=1
v=20 mV/s

		Iap(A)	Idp(A)	Dap(cm^2/sec)	Dcp(cm^2/sec)
1 layer	1 M HCl	0.00154	-0.00203	3.58E-13	6.22E-13
	1M H_2SO_4	0.00971	0.001424	1.44E-13	3.09E-13
	0.1 M LiClo4	0.000293	-0.00039	1.31E-10	2.36E-10
	1 M HCl Gel	0.001041	-0.00082	1.65E-11	1.04E-11
	1 M HCl PVA	0.00143	-0.0011	3.04E-11	1.83E-11

Table 9 (continued)

2 layers	1 M HCl	0.002113	-0.00235	6.80E-11	8.38E-11
	1M H_2SO_4	3.18E-03	-3.92E-03	1.54E-10	2.43E-10
	0.1 M $LiClO_4$	0.001061	-0.0014	1.72E-09	2.98E-09
	1 M HCl Gel	0.004252	-0.00303	2.76E-10	1.40E-10
	1 M HCl PVA	0.005043	-0.0037	3.88E-10	2.09E-10
3 layers	1 M HCl	0.014973	-0.01284	3.42E-09	2.51E-09
	1M H_2SO_4	0.00818	-0.00879	1.02E-09	1.18E-09
	0.1 M $LiClO_4$	0.001494	-0.00166	3.40E-09	4.21E-09
	1 M HCl Gel	0.00645	-0.00473	3.80E-09	2.04E-09
	1 M HCl PVA	0.017576	-0.01399	4.71E-09	2.98E-09

5.2.2 Chronoamperometry

5.2.2.1 Different Acids

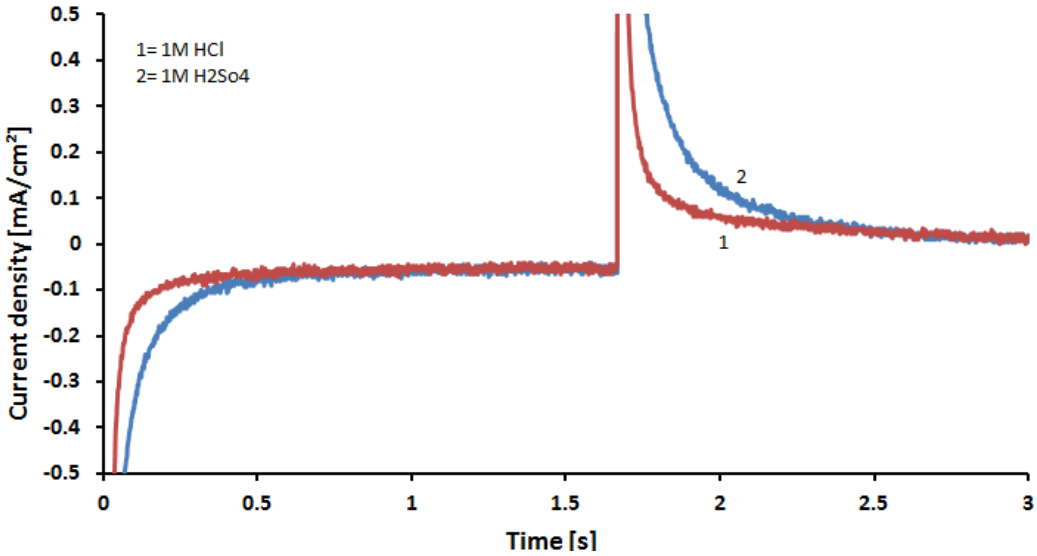

Figure 59 Chronoamperometry for 2 layer PANI in different acidic medium.

5.2.2.2 Different Gel Consistency

PANI film has been studied in two types of gel electrolytes synthesized. The gelatin electrolyte and polyvinyl alcohol gelatin semi-solid electrolyte has been used to study the chronoamperometric studies of polyaniline films. Interestingly, both oxidation and reduction of polyaniline film at two different gels show similar characteristics as shown in figure 60. The conductivity of gel plays an important role in transfer of the ion/electron from electrolyte/polymer films. The films showed similar current densities results; hence the nature of both studied electrolytes do not does affect the chronoamperometry redox properties of the films.

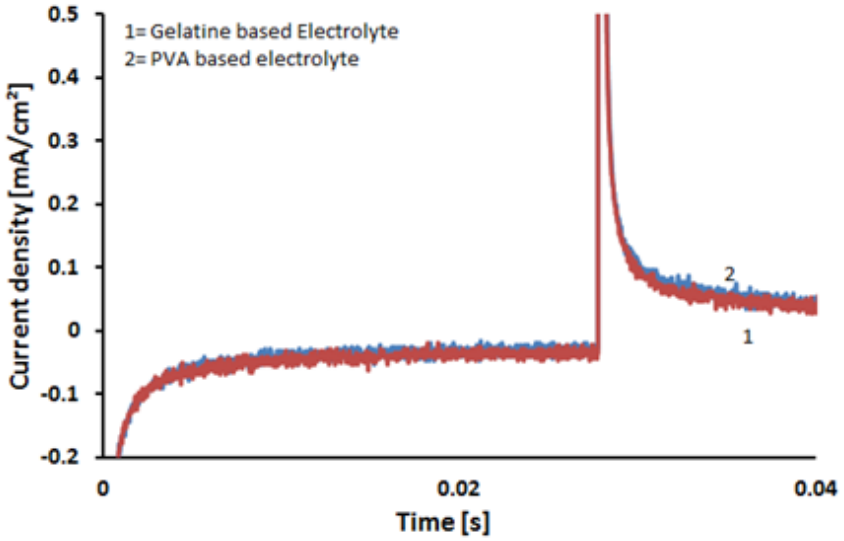

Figure 60 Chronoamperometry for layers PANI in different electrolyte consistencies.

5.2.2.3 Comparison to Different Thickness

The chronoamperometric study has been performed for different polyaniline film thickness. Figure 61 shows the chronoamperometric studies obtained for 1 layer, 2 layers, and 3 layers PANI. The current density increases as the film thickness increases from 1 to 3 layered polyaniline film, which is due to the increase of the conductivity of the film.

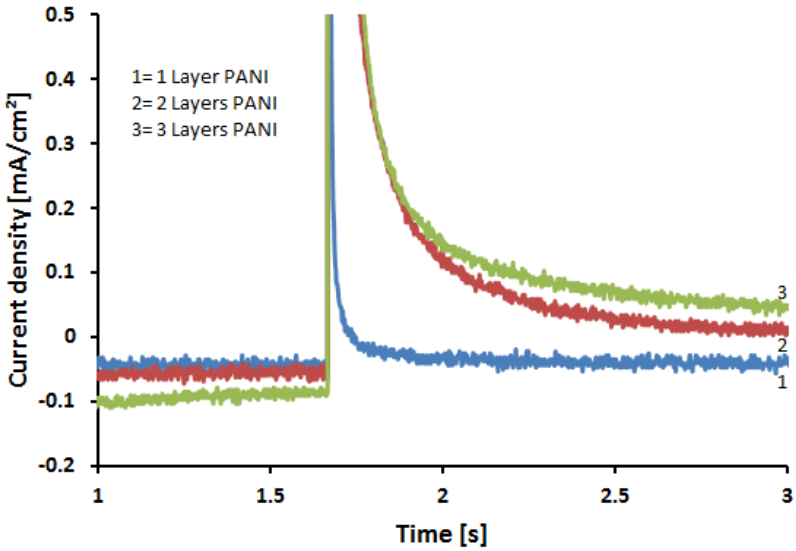

Figure 61 Chronoamperometry for different thickness PANI.

5.2.3 Electrochemical Impedance Spectroscopy

EIS was carried in a three-point electrode similar to the one used in CV in an electrolytic cell of 1 M HCl in a frequency range of 100 kHz to 100 mHz. Two graphs were extracted from this spectroscopy: Nyquist plot and Bode plot. These graphs show a capacitance behavior of the PANI thin films. Figure 62 shows the equivalent circuit obtained, which corresponds the Randles cell [66]. Rs corresponds to the resistance of the electrolyte solution calculated between the reference electrode and the surface of the thin film. The capacitance CPE corresponds to the capacitance of the thin film. Finally, Rp represents the resistance of the thin film, which changes with different thickness. Note that the introduction of CPE comparing to a pure capacitance circuit is more appropriate to describe the AC response of PANI thin film [82]. Table 10 summarizes all the parameters obtained from the best fitting of the equivalent circuit for different PANI films, which is shown in Figure 62. It can be concluded that the PANI films have a pseudo-capacitance behavior.

Figure 63 shows Nyquist plot for 1 layer, 2 layer, and 3 layers, and using equation $C=(2\pi f^{*}Z)^{-1}$ from the Bode Plot (figure 64), the capacitance increases with increasing film thickness, because the material tends to store more ionic charges.

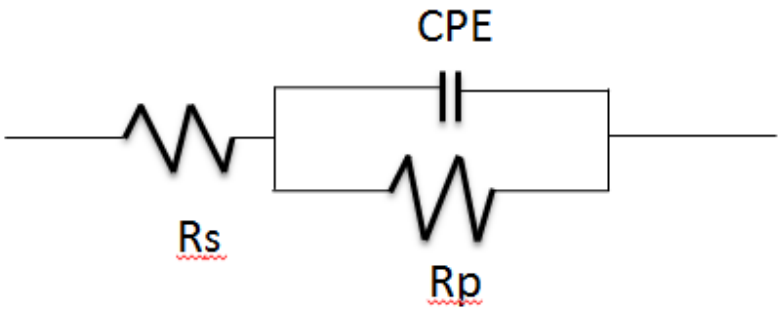

Figure 62 Equivalent circuit obtained from the best fitting.

Figure 63 shows Nyquist plot for 1 layer, 2 layer, and 3 layers, and using equation $C=(2\pi f^{*}Z)^{-1}$ from the Bode Plot (figure 64), the capacitance increases with increasing film thickness, because the material tends to store more ionic charges.

Table 10 Parameters extracted from the best fitting of the equivalent circuit for different PANI films.

Parameters	1 Layer PANI	2 Layer PANI	3 Layer PANI	PB/PANI	Rhodamine B/PANI
R_p (ohms)	$145*10^{3}$	$130.9*10^{3}$	$203*10^{3}$	$7.506*10^{3}$	$144*10^{6}$
R_s(ohms)	8.492	15.97	15.14	76.57	11.56
Y_0=C (F)	$4.7*10^{-3}$	$12.51*10^{-3}$	$13.96*10^{-2}$	$18.98*10^{-3}$	$5.51*10^{-3}$
α	$958.3*10^{-3}$	$967.9*10^{-3}$	$957*10^{-3}$	$956*10^{-3}$	$830.3*10^{-3}$
Goodness of Fit	$2.519*10^{-3}$	$554*10^{-6}$	$857.7*10^{-6}$	$1.8*10^{-3}$	$11.17*10^{-3}$

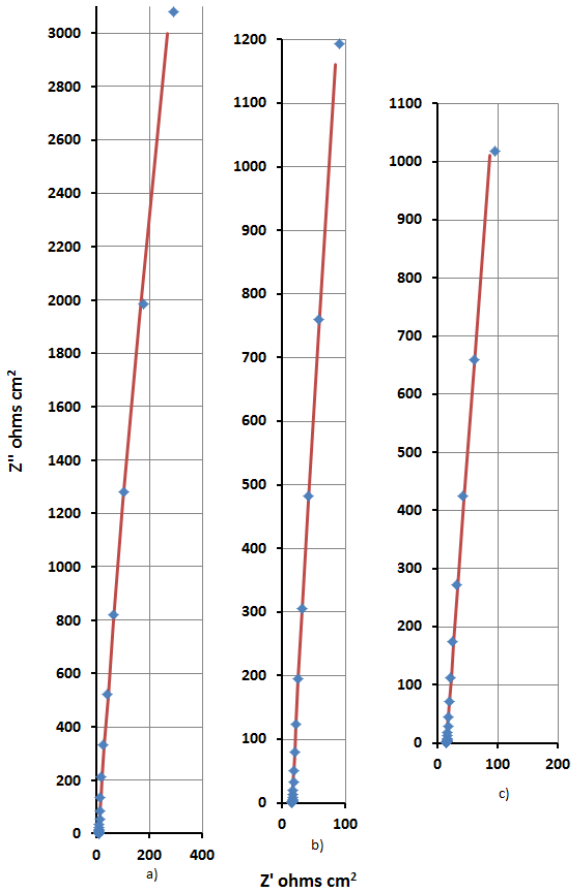

Figure 63 Nyquist plot for different thicknesses PANI. a)1 layer PANI b)2 layers PANI c)3 layers PANI.

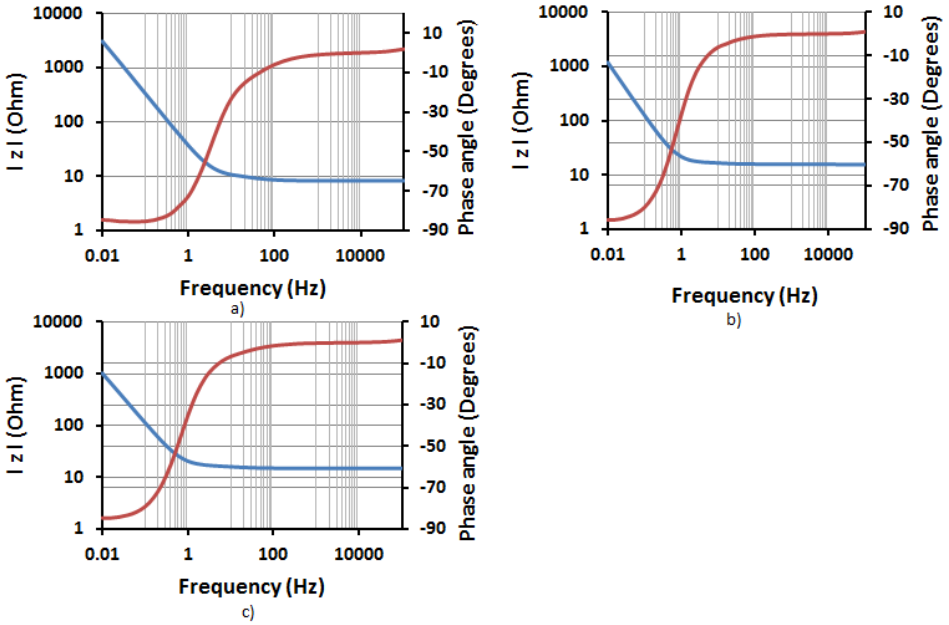

Figure 64 Bode plot for different thicknesses PANI. a)1 layer PANI b)2 layer PANI c)3 layer PANI.

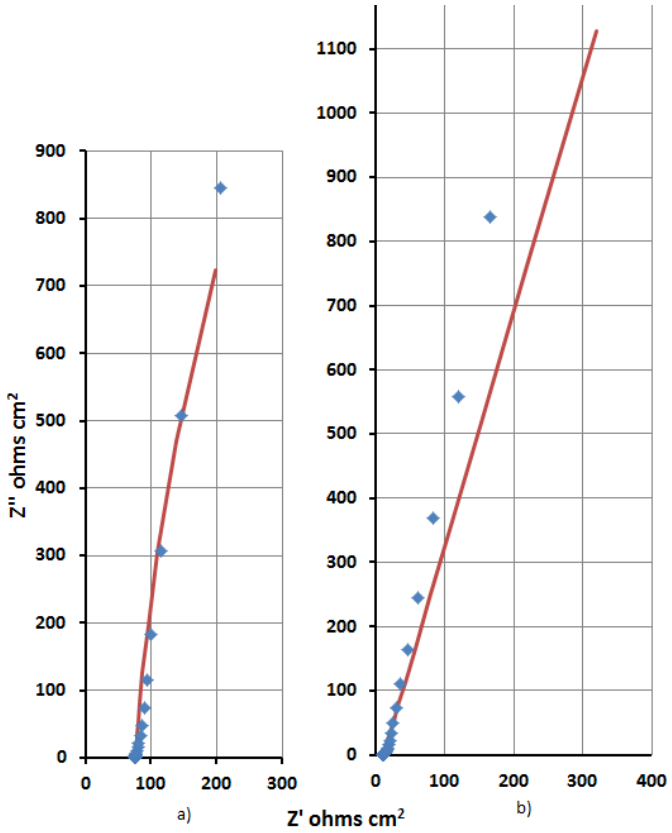

Figure 65 Nyquist plot for dye incorporated PANI. a)PB/PANI b)Rhodamine B/PANI.

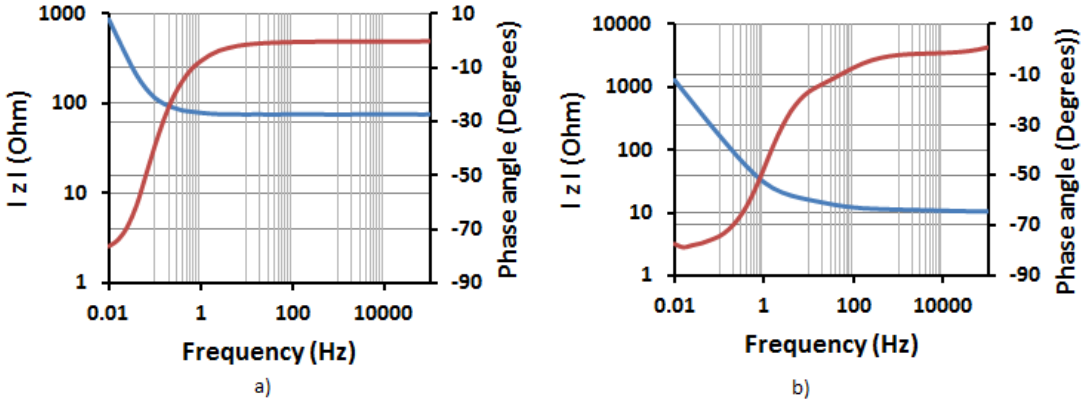

Figure 66 Bode plot for dye incorporated a) PB/PANI b) RhB/PANI.

Figure 65 shows the Nyquist plot for RhB/PANI and PB/PANI. The capacitance of PB/PANI is higher than the one observed for the different thicknesses of PANI. On the other hand, RB/PANI has a smaller capacitance than PB/PANI, but a higher capacitance than the one observed with 1

layer PANI. As mentioned, PB is a metal hexacyanoferrate, which is why it causes the PB/PANI to have a higher capacitance than the 2 layer PANI film. On the other hand, RB/PANI used a different deposition method. Rhodamine B certainly decreases the conductivity, but allows better charge transfer in RB/PANI film.

Note that all the Bode plots show a transition from ideally capacitive at a low frequency range, which is represented by the straight line at the phase angle of 45º, to resistive behavior at a high frequency range. The ideally capacitive region can be explained by an ion diffusion in in porous structure of polyaniline film [83, 84].

CHAPTER 6. CONCLUSION

Five different films (1 layer, 2 layers, 3 layers PANI, and dyes incorporated films with Prussian Blue and Rhodamine B) were synthesized, characterized, and investigated their electrochemical properties. The different thicknesses of PANI were synthesized using the in-situ self-assembly technique. The dye PB was electrodeposited on 2-layer in-situ self-assembled PANI layer, whereas Rhodamine B/PANI was deposited on plain FTO glass using electrochemical deposition. For the 1 layer, 2 layers, and 3 layers PANI, the peaks in the UV spectra was used to study the electronic properties and calculate the thickness of the films. The UV spectra behavior of the films was similar with an increase of film thickness; however, the UV-vis spectra of PB/PANI and RhB/PANI displayed different peak locations, since different deposition techniques have been used with an incorporation of the dyes. FTIR spectra of polyaniline film fabricated by self-assembly or electrochemical techniques showed similar characteristics. However, PB/PANI had an extra peak at 2050 cm^{-1}, which corresponds to the Fe-CN stretching mode in the cyanometallate lattice, due to the presence of PB. SEM images for the 1 layer PANI showed a compact PANI layer, but as the thickness grew PANI became fiber-like. The same behavior was noticed for the dye incorporated films. This fiber-like behavior is explained by having polyaniline and its oligomers simultaneaously deposited on the substrate. XRD results for 1 layer and 2 layers PANI displayed no apparent peaks, indicating its amorphous nature; however, as the film grew, the thin film exhibited three peaks, which is due to the polycrystalline structure of the thicker film. Moreover, an extra peak was noticeable in the PB/PANI, indicating the crystallinity of the dye. Two different set up of I-V characteristics were studied: a lateral and

an across set-up. The lateral set-up consisted of taping two copper foils on top of the PANI films, and the across set up consisted of taping one copper tape on PANI and the other on glass. It was noticed that the I-V characteristics for the lateral set-up and across set-up showed a nearly Ohmic behavior. It was shown through cyclic voltammetry that 1 layer PANI showed the fastest electroactive switching and reversible properties from transparent to dark blue in 1 M HCl compared to other PANI thicknesses for the same potential range. This is due to the fact that the increase in number of layers decreases the rate of intercalation/deintercalation of acid ions with polyaniline films. The reversibility was shown by studying the cyclic voltammetry indicating a higher working potential displayed by HCl. This is also shown in the chronoamperometric studies as 1 M HCl showed higher current density vs. time comparing to the chronoamperometric studies displayed by H_2SO_4. This is due to SO_4^{2-} being larger in size and having a bigger charge than Cl^-. Moreover, over time, the current density increases as the film thickness grew, which is due to an increase of conductivity as more layers are added. The current density stayed the same for similar concentration in different gel consistencies (gelatin vs. PVA) for the chronoamperometric studies. However, the change in the electrolyte's consistency, from liquid to semi-solid, did change the electrochemical properties of the film , as the PVA and gelatin moleculars' structure interfered with the transfer of ions to the electrode. Finally, in the EIS, it was shown that these PANI thin films exhibit a pseudo-capacitance behavior, and as the film thickness grew, the capacitance increased. PB/PANI has a higher capacitance than the 2 layers of PANI film; whereas, RhB/PANI has a capacitance value that lies between the 1 layer PANI and 2 layer PANI. This is due to PB being a hexacyanoferrate material, which increases the capacitance of the electrode

CHAPTER 7. FUTURE RECOMMENDATION

This thesis concentrated on the studies of polyaniline as a single electrode for the application of electrochromic device. Instead, the whole performance and properties of the device can be studied. Also, only two dyes have been used, but copolymerization between PANI and another polymer, nanoparticles, or different dye (merocyanine, phthalocyanine, congo red, etc.) could be used, which will broaden our color spectrum or improve the electrode. HCl and H_2SO_4 were used as protonic acid along with Gelatin and PVA based electrolyte. Other acids can be studied, and instead of only studying liquid and semisolid electrolytes, a solid electrolyte can be used to study the electrochemical properties of the film. This can help decide which electrolyte will perform the fastest switching property.

REFERENCES

1. Chiang, C., et al., *Synthesis of highly conducting films of derivatives of polyacetylene,(CH) x.* Journal of the American Chemical Society, 1978. 100(3): p. 1013-1015.
2. John, R., *Electrochemical Studies of heterocyclic Conducting Polymers*, in *Department of Chemistry*. 1992, University of Wollongong. p. 294.
3. Yang, X., *Semiconducting Polymer Composites: Principles, Morphologies, Properties and Applications*. 2012: Wiley.
4. Wang, Y. and X. Jing, *Intrinsically conducting polymers for electromagnetic interference shielding.* Polymers for advanced technologies, 2005. 16(4): p. 344-351.
5. Heeger, A.J., A.G. MacDiarmid, and P.J. Nigrey, *Electrochemical doping of conjugated polymers*. 1982, Google Patents.
6. Mastragostino, M., C. Arbizzani, and F. Soavi, *Polymer-based supercapacitors.* Journal of Power Sources, 2001. 97: p. 812-815.
7. McQuade, D.T., A.E. Pullen, and T.M. Swager, *Conjugated polymer-based chemical sensors.* Chemical Reviews, 2000. 100(7): p. 2537-2574.
8. Di, W. and A. Ivaska, *Electrochemical biosensors based on polyaniline.* Chemia analityczna, 2006. 51(6): p. 839-852.
9. Xu, J., et al., *Organic-inorganic nanocomposites via directly grafting conjugated polymers onto quantum dots.* Journal of the American Chemical Society, 2007. 129(42): p. 12828-12833.
10. Burroughes, J., et al., *Light-emitting diodes based on conjugated polymers.* nature, 1990. 347(6293): p. 539-541.
11. Beaujuge, P.M. and J.R. Reynolds, *Color control in π-conjugated organic polymers for use in electrochromic devices.* Chemical reviews, 2010. 110(1): p. 268-320.
12. Ndangili, P.M., et al., *Electronics of Conjugated Polymers (I): Polyaniline.* 2012.
13. Ansari Khalkhali, R., *Electrochemical Synthesis and Characterization of Electroactive Conducting Polypyrrole Polymers.* Russian Journal of Electrochemistry, 2005. 41(9): p. 950-955.
14. Bredas, J.L. and G.B. Street, *Polarons, bipolarons, and solitons in conducting polymers.* Accounts of Chemical Research, 1985. 18(10): p. 309-315.
15. Natta, G., G. Mazzanti, and P. Corradini, *Atti Accad. Naz. Lincei, Cl.* Sci. Fis. Mat. Nat., Rend, 1958. 25(3).
16. Ito, T., H. Shirakawa, and S. Ikeda, *Simultaneous polymerization and formation of polyacetylene film on the surface of concentrated soluble Ziegler-type catalyst solution.* Journal of polymer science: polymer chemistry edition, 1974. 12(1): p. 11-20.
17. Chiang, C.K., et al., *Electrical conductivity in doped polyacetylene.* Physical Review Letters, 1977. 39(17): p. 1098.

18. Naarmann, H. and N. Theophilou, *New process for the production of metal-like, stable polyacetylene.* Synthetic Metals, 1987. 22(1): p. 1-8.
19. Saxman, A., R. Liepins, and M. Aldissi, *Polyacetylene: its synthesis, doping and structure.* Progress in polymer science, 1985. 11(1): p. 57-89.
20. Wise, D.L., *Electrical and Optical Polymer Systems: Fundamentals: Methods, and Applications*. Vol. 45. 1998: CRC Press.21. Jolivet, M., et al., *Morphology, dopant concentration, and electrical properties of H2SO4- and BiCl3-doped polyacetylene films.* physica status solidi (a), 1984. 82(1): p. 257-263.
22. Bolto, B.A., R. McNeill, and D. Weiss, *Electronic conduction in polymers. III. Electronic properties of polypyrrole.* Australian Journal of Chemistry, 1963. 16(6): p. 1090-1103.
23. Diaz, A. and B. Hall, *Mechanical properties of electrochemically prepared polypyrrole films.* IBM Journal of Research and Development, 1983. 27(4): p. 342-347.
24. Patois, T., et al., *Characterization of the surface properties of polypyrrole films: Influence of electrodeposition parameters.* Synthetic Metals, 2011. 161(21): p. 2498-2505.
25. Kudoh, Y., M. Fukuyama, and S. Yoshimura, *Stability study of polypyrrole and application to highly thermostable aluminum solid electrolytic capacitor.* Synthetic metals, 1994. 66(2): p. 157-164.
26. Ko, J., et al., *Morphology and electrochemical properties of polypyrrole films prepared in aqueous and nonaqueous solvents.* Journal of the Electrochemical Society, 1990. 137(3): p. 905-909.
27. Qi, G., L. Huang, and H. Wang, *Highly conductive free standing polypyrrole films prepared by freezing interfacial polymerization.* Chemical Communications, 2012. 48(66): p. 8246-8248.
28. Abdulla, H.S. and A.I. Abbo, *Optical and electrical properties of thin films of polyaniline and polypyrrole.* Int J Electrochem Sci, 2012. 7: p. 10666-10678.
29. Fonner, J.M., et al., *Biocompatibility implications of polypyrrole synthesis techniques.* Biomedical materials, 2008. 3(3): p. 034124.
30. Slimane, A.B., M.M. Chehimi, and M.-J. Vaulay, *Polypyrrole-coated poly (vinyl chloride) powder particles: surface chemical and morphological characterisation by means of X-ray photoelectron spectroscopy and scanning electron microscopy.* Colloid and Polymer Science, 2004. 282(4): p. 314-323.
31. Yeu, T., et al., *Electrochemical characterization of electronically conductive polypyrrole on cyclic voltammograms.* Journal of The Electrochemical Society, 1991. 138(10): p. 2869-2877.
32. Yamamoto, T., K. Sanechika, and A. Yamamoto, *Preparation of thermostable and electric-conducting poly (2, 5-thienylene).* Journal of Polymer Science: Polymer Letters Edition, 1980. 18(1): p. 9-12.
33. Lin, J.W.P. and L.P. Dudek, *Synthesis and properties of poly (2, 5-thienylene).* Journal of Polymer Science: Polymer Chemistry Edition, 1980. 18(9): p. 2869-2873.
34. McCullough, R.D., et al., *Self-orienting head-to-tail poly (3-alkylthiophenes): new insights on structure-property relationships in conducting polymers.* Journal of the American Chemical Society, 1993. 115(11): p. 4910-4911.
35. Kitao, S., et al., *Mössbauer study of iodine-doped polythiophene and poly (3-Methylthiophene).* Hyperfine Interactions, 1994. 93(1): p. 1439-1444.

36. Frommer, J.E., *Conducting polymer solutions.* Accounts of Chemical Research, 1986. 19(1): p. 2-9.
37. Kelkar, D. and A. Chourasia, *Structural properties of polythiophene doped with FeCl3.* 2011.
38. Skotheim, T.A., *Handbook of conducting polymers*. 1997: CRC press.
39. Patil, B., A. Jagadale, and C. Lokhande, *Synthesis of polythiophene thin films by simple successive ionic layer adsorption and reaction (SILAR) method for supercapacitor application.* Synthetic Metals, 2012. 162(15): p. 1400-1405.
40. Letheby, H., *XXIX.—On the production of a blue substance by the electrolysis of sulphate of aniline.* J. Chem. Soc., 1862. 15: p. 161-163.
41. Green, A.G. and A.E. Woodhead, *CXVII.-Aniline-black and allied compounds. Part II.* Journal of the Chemical Society, Transactions, 1912. 101(0): p. 1117-1123.
42. Michira, I., et al. *Synthesis, characterisation of novel polyaniline nanomaterials and application in amperometric biosensors*. in *Macromolecular symposia*. 2007. Wiley Online Library.
43. Masters, J., et al., *Polyaniline: allowed oxidation states.* Synthetic Metals, 1991. 41(1): p. 715-718.
44. Rajapakse, R., A.C. Perera, and H. Premasiri, *Polyaniline retained glass templates as sensors for acidic/basic and/or redox gases.* Journal of the National Science Foundation of Sri Lanka, 2000. 28(4): p. 277-285.
45. Sapurina, I., A. Riede, and J. Stejskal, *In-situ polymerized polyaniline films: 3. Film formation.* Synthetic Metals, 2001. 123(3): p. 503-507.
46. Zotti, G., S. Cattarin, and N. Comisso, *Cyclic potential sweep electropolymerization of aniline: The role of anions in the polymerization mechanism.* Journal of electroanalytical chemistry and interfacial electrochemistry, 1988. 239(1): p. 387-396.
47. Wallace, G.G., et al., *Conductive electroactive polymers: intelligent polymer systems*. 2008: CRC press.
48. Yilmaz, F., *Polyaniline: Synthesis, Characterization, solution properties and composites*, in *Natural and Applied Sciences*. 2007, Middle East Technical University. p. 148.
49. Huang, W. and A. MacDiarmid, *Optical properties of polyaniline.* Polymer, 1993. 34(9): p. 1833-1845.
50. Tallman, D.E., et al., *Electroactive conducting polymers for corrosion control.* Journal of Solid State Electrochemistry, 2002. 6(2): p. 73-84.
51. Soto-Oviedo, M.A., et al., *Antistatic coating and electromagnetic shielding properties of a hybrid material based on polyaniline/organoclay nanocomposite and EPDM rubber.* Synthetic metals, 2006. 156(18): p. 1249-1255.
52. Karami, H., M.F. Mousavi, and M. Shamsipur, *A new design for dry polyaniline rechargeable batteries.* Journal of Power Sources, 2003. 117(1): p. 255-259.
53. Sapurina, I.Y. and M. Shishov, *Oxidative Polymerization of Aniline: Molecular Synthesis of Polyaniline and the Formation of Supramolecular Structures.* 2012.
54. Zhang, K., et al., *Graphene/polyaniline nanofiber composites as supercapacitor electrodes.* Chemistry of Materials, 2010. 22(4): p. 1392-1401.
55. Kitani, A., M. Kaya, and K. Sasaki, *Performance study of aqueous polyaniline batteries.* Journal of The Electrochemical Society, 1986. 133(6): p. 1069-1073.
56. Wessling, B. and J. Posdorfer, *Corrosion prevention with an organic metal (polyaniline): corrosion test results.* Electrochimica Acta, 1999. 44(12): p. 2139-2147.

57. Monk, P.M., R.J. Mortimer, and D.R. Rosseinsky, *Electrochromism and electrochromic devices*. Vol. 421. 2007: Cambridge University Press Cambridge, UK.
58. Skoog, D.A. and D.M. West, *Principles of instrumental analysis*. Vol. 158. 1980: Saunders College Philadelphia.
59. Nicolet, T., *Introduction to fourier transform infrared spectrometry.* Information booklet, 2001.
60. Leng, Y., *Materials characterization: introduction to microscopic and spectroscopic methods*. 2013: John Wiley & Sons.
61. Zanello, P., *Inorganic electrochemistry: theory, practice and applications*. 2003: Royal Society of Chemistry.
62. Koryta, J., J. Dvorak, and A.M. Bond, *Principles of electrochemistry: Wiley, New York, 1987 (ISBN 0-471-91211-5). xi+ 447 pp. Price£ 49.50*. 1987, Elsevier.
63. Compton, R.G. and C.E. Banks, *Understanding voltammetry*. 2007: World Scientific.
64. Lasia, A., *Electrochemical Impedance Spectroscopy and its Applications*, in *Modern Aspects of Electrochemistry*, B.E. Conway, J.O.M. Bockris, and R. White, Editors. 2002, Springer US. p. 143-248.
65. Jüttner, K., *Electrochemical impedance spectroscopy (EIS) of corrosion processes on inhomogeneous surfaces.* Electrochimica Acta, 1990. 35(10): p. 1501-1508.
66. Loveday, D., P. Peterson, and B. Rodgers, *Evaluation of organic coatings with electrochemical impedance spectroscopy.* JCT coatings tech, 2004. 8: p. 46-52.
67. Li, H., X. Huang, and L. Chen, *Electrochemical impedance spectroscopy study of SnO and nano-SnO anodes in lithium rechargeable batteries.* Journal of Power Sources, 1999. 81: p. 340-345.
68. Ivers-Tiffée, E., A. Weber, and H. Schichlein, *Electrochemical impedance spectroscopy.* Handbook of fuel cells, 2010.
69. Love, J.C., et al., *Self-assembled monolayers of thiolates on metals as a form of nanotechnology.* Chemical reviews, 2005. 105(4): p. 1103-1170.
70. Stejskal, J. and I. Sapurina, *Polyaniline: Thin films and colloidal dispersions (IUPAC Technical Report).* Pure and Applied Chemistry, 2005. 77(5): p. 815-826.
71. Misra, S., et al., *Preparation and characterization of vacuum deposited semiconducting nanocrystalline polymeric thin film sensors for detection of HCl.* Polymer, 2004. 45(25): p. 8623-8628.
72. Saikia, P.J. and P.C. Sarmah, *Investigation of Polyaniline Thin Film and Schottky Junction with Aluminium for Electrical and Optical Characterization.* Materials Sciences and Applications, 2011. 2: p. 1022.
73. Li, X., et al., *Process for Preparing Macroscopic Quantities of Brightly Photoluminescent Silicon Nanoparticles with Emission Spanning the Visible Spectrum.* Langmuir, 2003. 19(20): p. 8490-8496.
74. Smart, P. and I. Laidlaw, *An evaluation of some fluorescent dyes for water tracing.* Water Resources Research, 1977. 13(1): p. 15-33.
75. Ebrahim, S., et al., *Dye-Sensitized Solar Cell Based on Polyaniline/Multiwalled Carbon Nanotubes Counter Electrode*. International Journal of Photoenergy, 2013. 2013.
76. Karstens, T. and K. Kobs, *Rhodamine B and rhodamine 101 as reference substances for fluorescence quantum yield measurements.* The Journal of Physical Chemistry, 1980. 84(14): p. 1871-1872.

77. Dunbar, K.R. and R.A. Heintz, *Chemistry of Transition Metal Cyanide Compounds: Modern Perspectives*, in *Progress in Inorganic Chemistry*. 2007, John Wiley & Sons, Inc. p. 283-391.
78. Thakur, B. and S.N. Sawant, *Polyaniline/Prussian-Blue-Based Amperometric Biosensor for Detection of Uric Acid.* ChemPlusChem, 2013. 78(2): p. 166-174.
79. Leventis, N. and Y.C. Chung, *Polyaniline-prussian blue novel composite material for electrochromic applications.* Journal of The Electrochemical Society, 1990. 137(10): p. 3321-3322.
80. Zhang, X., et al., *Preparation, characterization, and property of polyaniline/Prussian blue micro-composites in a low-temperature hydrothermal process.* Applied Surface Science, 2007. 253(22): p. 9030-9034.
81. Shim, Y.B., M.S. Won, and S.M. Park, *Electrochemistry of conductive polymers VIII in situ spectroelectrochemical studies of polyaniline growth mechanisms.* Journal of The Electrochemical Society, 1990. 137(2): p. 538-544.
82. Rammelt, U. and G. Reinhard, *On the applicability of a constant phase element (CPE) to the estimation of roughness of solid metal electrodes.* Electrochimica Acta, 1990. 35(6): p. 1045-1049.
83. Arabale, G., et al., *Enhanced supercapacitance of multiwalled carbon nanotubes functionalized with ruthenium oxide.* Chemical Physics Letters, 2003. 376(1): p. 207-213.
84. Patil, D., et al., *Chemical synthesis of highly stable PVA/PANI films for supercapacitor application.* Materials Chemistry and Physics, 2011. 128(3): p. 449-455.

APPENDICES

Appendix A Copyright Permissions

Below is permission for the use of Figure 1, 4, 13, 16, and 17.

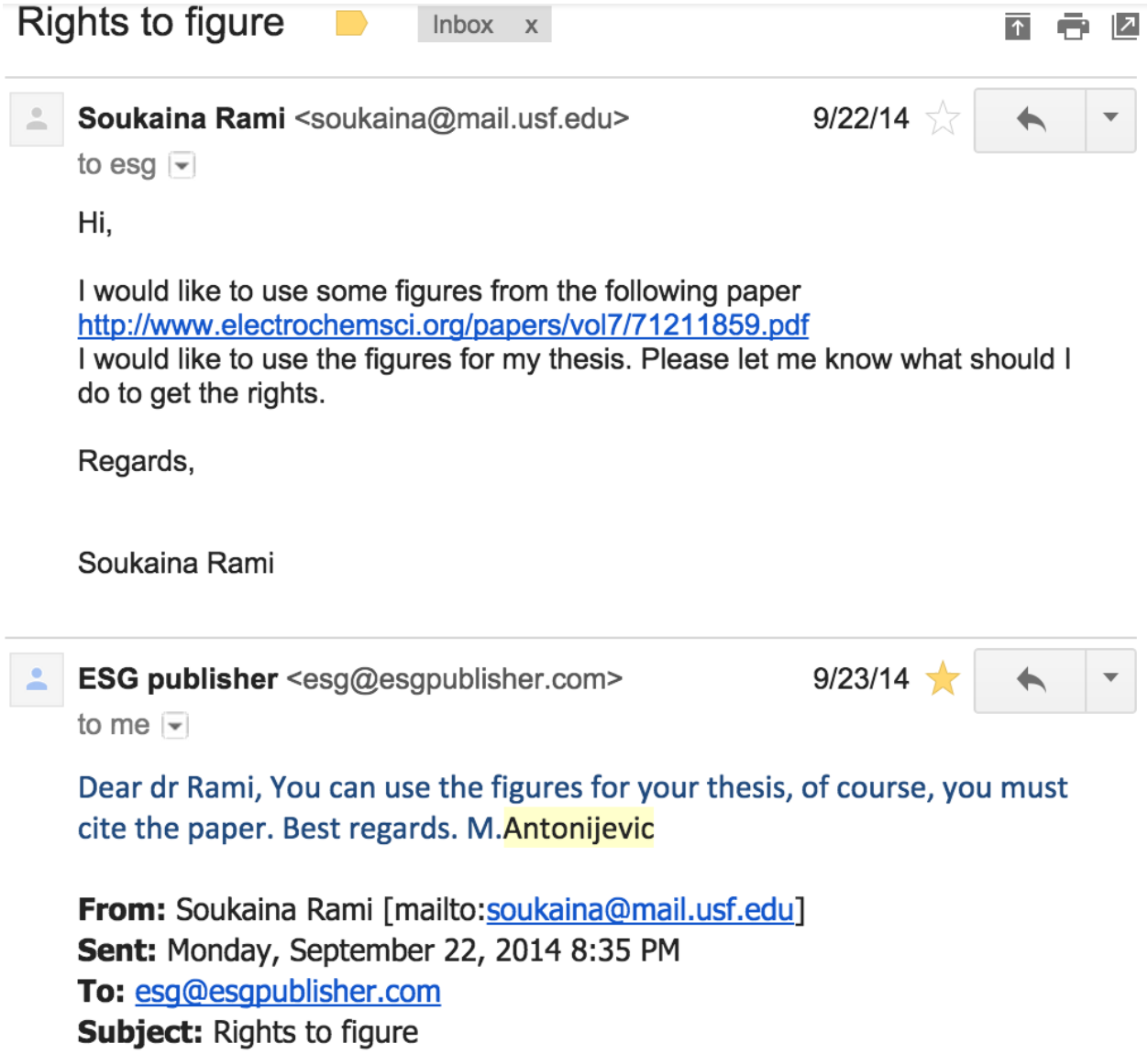

Rights to figure

Inbox x

Soukaina Rami <soukaina@mail.usf.edu> 9/22/14

to esg

Hi,

I would like to use some figures from the following paper
http://www.electrochemsci.org/papers/vol7/71211859.pdf
I would like to use the figures for my thesis. Please let me know what should I do to get the rights.

Regards,

Soukaina Rami

ESG publisher <esg@esgpublisher.com> 9/23/14

to me

Dear dr Rami, You can use the figures for your thesis, of course, you must cite the paper. Best regards. M.Antonijevic

From: Soukaina Rami [mailto:soukaina@mail.usf.edu]
Sent: Monday, September 22, 2014 8:35 PM
To: esg@esgpublisher.com
Subject: Rights to figure

Below is permission for the use of figure 2.

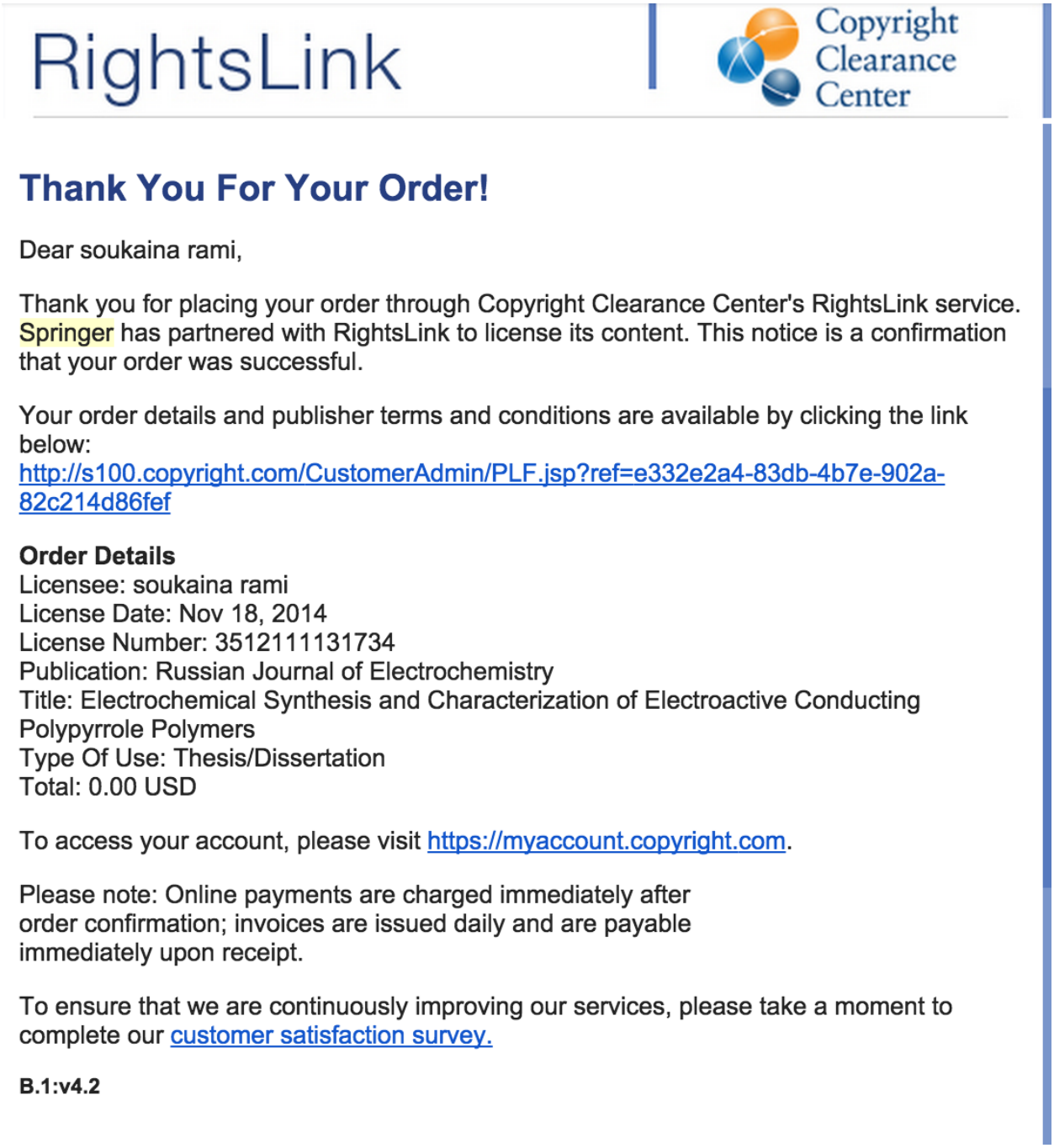

RightsLink | Copyright Clearance Center

Thank You For Your Order!

Dear soukaina rami,

Thank you for placing your order through Copyright Clearance Center's RightsLink service. Springer has partnered with RightsLink to license its content. This notice is a confirmation that your order was successful.

Your order details and publisher terms and conditions are available by clicking the link below:
http://s100.copyright.com/CustomerAdmin/PLF.jsp?ref=e332e2a4-83db-4b7e-902a-82c214d86fef

Order Details
Licensee: soukaina rami
License Date: Nov 18, 2014
License Number: 3512111131734
Publication: Russian Journal of Electrochemistry
Title: Electrochemical Synthesis and Characterization of Electroactive Conducting Polypyrrole Polymers
Type Of Use: Thesis/Dissertation
Total: 0.00 USD

To access your account, please visit https://myaccount.copyright.com.

Please note: Online payments are charged immediately after order confirmation; invoices are issued daily and are payable immediately upon receipt.

To ensure that we are continuously improving our services, please take a moment to complete our customer satisfaction survey.

B.1:v4.2

Below is permission for the use of figure 3.

Soukaina Rami <soukaina@mail.usf.edu> 11/20/14

to permissions

Hi,

i would like to use figure 17.1 from the book:
Yang, X., *Semiconducting Polymer Composites: Principles, Morphologies, Properties and Applications*. 2012: Wiley.
in my thesis. How do I do to request the rights to use a figure from a book?

Regards,

Soukaina Rami

Rights DE <RIGHTS-and-LICENCES@wiley-vch.de> 11/24/14

to Rights, me

Dear Soukaina Rami,

We hereby grant permission for the requested use expected that due credit is given to the original source.

If material appears within our work with credit to another source, authorisation from that source must be obtained.

Credit must include the following components:

- Books: Author(s)/ Editor(s) Name(s): Title of the Book. Page(s). Publication year. Copyright Wiley-VCH Verlag GmbH & Co. KGaA. Reproduced with permission.

- Journals: Author(s) Name(s): Title of the Article. Name of the Journal. Publication year. Volume. Page(s). Copyright Wiley-VCH Verlag GmbH & Co. KGaA. Reproduced with permission.

- Online Portal: Author(s): Title of the Online portal. Link or DOI. Publication year. Copyright Wiley-VCH Verlag GmbH & Co. KGaA. Reproduced with permission.

With kind regards

Heike Weller

Rights Manager

Rights & Licenses

Wiley-VCH Verlag GmbH & Co. KGaA

Boschstraße 12

69469 Weinheim

Below is permission for the use of figure 5.

Monika Oakman <moakman@uow.edu.au> 11/19/14

to me

Soukaina,

Thankyou for your request to use some figures from “Eletrochemical Studies of heterocyclic conducting polymers” by Richard John 1992 in your thesis.

We have been advised by our Copyright Officer that as the figures are being used in the your thesis, you are able to utilise the terms of Fair Use in order to include them. Attribution must however be given to the author.

Regards,

Monika Oakman
Monika Oakman
Scholarly Content Officer
Library
University of Wollongong NSW 2522
T + 61 2 4221 5109
W www.library.uow.edu.au

Below is permission for the use of figure 6.

Order Completed

Thank you for your order.

This Agreement between soukaina rami ("You") and John Wiley and Sons ("John Wiley and Sons") consists of your license details and the terms and conditions provided by John Wiley and Sons and Copyright Clearance Center.

Your confirmation email will contain your order number for future reference.

Get the printable license.

License Number	3544940629219
License date	Jan 09, 2015
Licensed Content Publisher	John Wiley and Sons
Licensed Content Publication	physica status solidi (a) applications and materials science
Licensed Content Title	Morphology, dopant concentration, and electrical properties of H2SO4- and BiCl3-doped polyacetylene films
Licensed Content Author	M. Jolivet,M. Cadene,J. M. Abadie,M. Rolland
Licensed Content Date	Feb 16, 2006
Licensed Content Pages	7
Type of use	Dissertation/Thesis
Requestor type	University/Academic
Format	Electronic
Portion	Figure/table
Number of figures/tables	1
Original Wiley figure/table number(s)	Figure 1
Will you be translating?	No
Title of your thesis / dissertation	Synthesis, Characterization, and Electrochromic properties of Polyaniline Thin films
Expected completion date	Jan 2015
Expected size (number of pages)	100
Requestor Location	soukaina rami 2308 w jetton ave TAMPA, FL 33629 United States Attn: soukaina rami
Billing Type	Invoice
Billing address	soukaina rami 2308 w jetton ave TAMPA, FL 33629 United States Attn: soukaina rami
Total	0.00 USD

Below is permission for the use of figure 7.

Request for Permission to Reproduce or Re-Publish ECS Material

Please fax this form to The Electrochemical Society (ECS), Attn: Permissions Requests, 1.609.730.0629. You may also e-mail your request to copyright@electrochem.org. Include all the information as required on this form. Please allow 3-7 days for your request to be processed.

I am preparing a (choose one): paper chapter book • thesis

entitled Synthesis, Characterization, and Electrochromic Properties of Polyaniline Thin Films

to be published by: University of South Florida

in an upcoming publication entitled:

I request permission to use the following material in the publication noted above, and request nonexclusive rights for all subsequent editions and in all foreign language translations for distribution throughout the world

Description of material to be used— Indicate what material you wish to use (figures, tables, text, etc.) and give the full bibliographic reference for the source publication. You may attach a separate list, organized by ECS title.

Figure 3 and figure 6 in "The Cyclic Voltammetry of Pristine, Isomerized, Deuterated, and Partially Hydrogenated P-Type" Polyacetylene" J. Electrochem Soc. 1987 volume 134, issue 9,2179-2187

Signature: [redacted] Date: 11/19/2014

Name soukanta rani

Address: 4202 E Fowler ave, tampa, fl

Telephone: 8523289980 Fax

E-mail soukanta@mail.usf.edu

Permission is granted to reproduce the above-referenced material. Please acknowledge the author(s) and publication title of the original material, and include the words: "Reproduced by permission of ECS — The Electrochemical Society."

Nov. 25, 2014
Date

[redacted]
Annie Goedkoop, Publications Production Director

Below is permission for the use of figure 8 and 21.

Soukaina <soukaina@mail.usf.edu> Jan 14 (8 days ago)

to ijes

Hi,

I have contacted the esg to get the right and permission to use a figure in my thesis manuscript, and I have gotten no response. I have to submit my manuscript next week, so please let me know what I should do.
The figures I want to use are Figure 11 A and B from the following paper http://www.electrochemsci.org/papers/vol7/71110666.pdf in my thesis dissertation called: " Synthesis, Characterization, and Electrochromic application of Polyaniline Thin Films".

Thank you,

Regards,

Soukaina Rami

International Journal of Electrochem Jan 14 (8 days ago)

to me

Dear dr Rami, You can use the figure and other tings from the paper for your scientific work. Best regards. M.Antonijevic

---

From: Soukaina [mailto:soukaina@mail.usf.edu]
Sent: Wednesday, January 14, 2015 9:33 PM
To: ijes@esgpublisher.com
Subject: RIGHTS and permission

...

Below is permission for the use of figure 9.

Request for Permission to Reproduce or Re-Publish ECS Material

Please fax this form to: The Electrochemical Society (ECS), Attn: Permissions Requests, 1.609.730.0629. You may also e-mail your request to: copyright@electrochem.org. Include all the information as required on this form. Please allow 3-7 days for your request to be processed.

I am preparing a (choose one) paper chapter book • thesis

entitled: Synthesis, Characterization, and Electrochromic Properties of Polyaniline Thin Films

to be published by: University of South Florida

in an upcoming publication entitled:

I request permission to use the following material in the publication noted above, and request nonexclusive rights for all subsequent editions and in all foreign language translations for distribution throughout the world.

Description of material to be used—Indicate what material you wish to use (figures, tables, text, etc.) and give the full bibliographic reference for the source publication. You may attach a separate list, organized by ECS title.

Figure 3 in "Electrochemical Characterization of Electronically Conductive Polypyrrolic on Cyclic Voltammograms" J. Electrochem Soc. 1991 Volume 138 issue 10, 2869-2877

Signature: [redacted] Date: 11/19/2014

Name: soukaina rami

Address: 4202 E fowler ave, Tampa, Fl

Telephone: 3523589980 Fax:

E-mail: soukaina@mail.usf.edu

Permission is granted to reproduce the above-referenced material. Please acknowledge the author(s) and publication title of the original material, and include the words: "Reproduced by permission of ECS — The Electrochemical Society."

Nov. 25, 2014
Date

[redacted]
Annie Goedkoop, Publications Production Director

Below is permission for the use of figure 10, 11, and 12.

This is a License Agreement between soukaina rami ("You") and Elsevier ("Elsevier") The license consists of your order details, the terms and conditions provided by Elsevier, and the payment terms and conditions.

License number	Reference confirmation email for license number
License date	Nov 18, 2014
Licensed content publisher	Elsevier
Licensed content publication	Synthetic Metals
Licensed content title	Synthesis of polythiophene thin films by simple successive ionic layer adsorption and reaction (SILAR) method for supercapacitor application
Licensed content author	B.H. Patil,A.D. Jagadale,C.D. Lokhande
Licensed content date	September 2012
Licensed content volume number	162
Licensed content issue number	15-16
Number of pages	6
Type of Use	reuse in a thesis/dissertation
Portion	figures/tables/illustrations
Number of figures/tables/illustrations	1
Format	electronic
Are you the author of this Elsevier article?	No
Will you be translating?	No
Title of your thesis/dissertation	Synthesis, Characterization, and Electrochemical applications of Polyaniline Thin Film
Expected completion date	Nov 2014
Elsevier VAT number	GB 494 6272 12
Billing Type	Invoice
Billing address	2308 w jetton ave
	TAMPA, FL 33629
	United States
Permissions price	0.00 USD
VAT/Local Sales Tax	0.00 USD / 0.00 GBP
Total	0.00 USD

Below is permission for the use of Table 2.

Uthpala Karunarathne <uthpalak@nsf.ac.lk> 11/13/14

to me

Dear Soukaina,

Thank you for contacting the Editorial Office.
You can use the Table in your thesis without any problem.

Please make sure that you properly cite the JNSF article in the references, any in other occasion you use it.

Best regards,

Uthpala Karunarathne

Scientific Officer (Editorial Office)
National Science Foundation,
47/5, Maitland Place, Colombo 07,
SRI LANKA.

Phone: +94(0) 112696771-3 Ext: 122
Fax: +94(0) 112694754

The full text of the JNSF can be accessed through Sri Lanka Journals Online: http://www.sljol.info/index.php/JNSFSL/index

---

From: Soukaina Rami [mailto:soukaina@mail.usf.edu]
Sent: Thursday, November 13, 2014 1:55 AM
To: jnsf@nsf.ac.lk; scumming@inasp.info
Subject: rights

Hi,

My name is Soukaina Rami, and I am a graduate mechanical engineering student at the University of South Florida. I would like to get the rights to use one of the table 1 published in the paper below in my thesis manuscript.
These are the papers informations:

Polyaniline retained glass templates as sensors for acidic basic and/or redox gases by R.M.G Rajapakse, et al. 2000 28(4)p.277-285

Regards,

Soukaina Rami

Below is permission for the use of figure 20.

Order Completed

Thank you very much for your order.

This is a License Agreement between soukaina rami ("You") and Elsevier ("Elsevier"). The license consists of your order details, the terms and conditions provided by Elsevier, and the payment terms and conditions.

Get the printable license.

License Number	3547131217397
License date	Jan 13, 2015
Licensed content publisher	Elsevier
Licensed content publication	Polymer
Licensed content title	Optical properties of polyaniline
Licensed content author	W.S. Huang,A.G. MacDiarmid
Licensed content date	May 1993
Licensed content volume number	34
Licensed content issue number	9
Number of pages	13
Type of Use	reuse in a thesis/dissertation
Portion	figures/tables/illustrations
Number of figures/tables/illustrations	1
Format	both print and electronic
Are you the author of this Elsevier article?	No
Will you be translating?	No
Original figure numbers	The different band gaps present in polyaniline redox states
Title of your thesis/dissertation	Synthesis, Characterization, and Electrochromic properties of Polyaniline Thin films
Expected completion date	Jan 2015
Estimated size (number of pages)	100
Elsevier VAT number	GB 494 6272 12
Permissions price	0.00 USD
VAT/Local Sales Tax	0.00 USD / 0.00 GBP
Total	0.00 USD

Below is permission for the use of figure 14, 15, 30.

Soukaina Rami <soukaina@mail.usf.edu> 9/23/14

to faris.yilmaz

Dr. Faris,

My name is Soukaina Rami, and I am a graduate mechanical engineering student at the University of South Florida. I came upon your thesis in the following link:
http://etd.lib.metu.edu.tr/upload/3/12608598/index.pdf
I would like to get rights to use some of your figures in my own thesis.

Thank you,

Regards,

Soukaina Rami

Faris Yilmaz <faris.yilmaz@yahoo.com> 9/23/14

to me

Dear Rami

Yes you can use any figure you need in case you mention the reference.

Regards
Faris

Sent from Yahoo Mail on Android

From:"Soukaina Rami" <soukaina@mail.usf.edu>
Date:Tue, Sep 23, 2014 at 19:56
Subject:right of figures